

## Synthesis of new anionic carbosilane dendrimers *via* thiol–ene chemistry and their antiviral behaviour†

Cite this: *Org. Biomol. Chem.*, 2014, **12**, 3222

Marta Galán,<sup>a,b</sup> Javier Sánchez Rodríguez,<sup>b,c</sup> José Luis Jiménez,<sup>b,c</sup> Miguel Relloso,<sup>b,d</sup> Marek Maly,<sup>e,f</sup> F. Javier de la Mata,<sup>\*a,b</sup> M. A. Muñoz-Fernández<sup>\*b,d</sup> and Rafael Gómez<sup>\*a,b</sup>

A synthetic strategy has been developed for the preparation of anionic carbosilane dendrimers bearing sulfonate or carboxylate groups at their periphery by means of thiol–ene chemistry. It offers significant advantages, such as milder reaction conditions, shorter reaction times and more facile purification methods, when compared with other synthetic protocols used previously, e.g. hydrosilylation followed by a Michael-type addition or azide–alkyne coupling reactions. Molecular dynamics simulations of the second generation anionic dendrimers addressing shape and size effects of the terminal groups and conformational variability indicated that the core eccentricity and flexibility might need to be taken into account for toxicity and interaction with viral and/or cellular receptors, respectively. The biocompatibility of anionic carbosilane dendrimers has been explored showing differences between silicon-cored and polyphenoxo-cored dendrimers. In addition, silicon-cored dendrimers achieved 85–90% of HIV inhibition without inducing inflammation or vaginal irritation in mice, which makes them likely candidates for readily available, good and safe topical vaginal microbicides against HIV.

Received 21st January 2014,  
Accepted 12th March 2014

DOI: 10.1039/c4ob00162a

www.rsc.org/obc

## Introduction

Since the discovery of AIDS in 1981, no effective treatment has been developed despite all the efforts of the scientific community. Nowadays, more than 35 million people live with AIDS with 2.3 million of new infections in 2012.<sup>1</sup> As for the current antiretroviral therapy (HAART), people's longevity has been increased but infection has not been eradicated.<sup>2</sup> Therefore, there is an urgency to find a way to reduce viral spreading. This is the reason why many researchers have focused their efforts on the synthesis and preparation of microbicides

capable of controlling the spread of the disease by interfering with earlier steps of the viral infection mechanism.<sup>3</sup> Microbicides are chemical entities that can prevent or reduce the transmission of AIDS and other STIs when applied to the vagina (or rectum), which allows for better disease control in women, who are the most vulnerable to infection. Many microbicide candidates are based on polyanionic compounds, which have the capacity to interact with the gp120 protein which is anchored to the viral envelope and is responsible for the binding to host cells, thus inhibiting the viral fusion process, a vital step in the viral replication cycle.<sup>4</sup> Several examples of this kind of chemicals can be found in the literature,<sup>5</sup> although VivaGel®, a polylysine-based dendrimer with naphthylsulfonate groups at the periphery, is currently the only agent to have made it as far as Phase III trials for HSV and Phase II trials for HIV.<sup>5e,6</sup>

Anionic dendrimers have been used as an alternative to polymers in many medical applications for their ability to present a highly functionalized surface without losing structural control.<sup>7</sup> Over the last few years, our research group has developed a number of anionic carbosilane dendrimers with sulfonate, sulfate or carboxylate groups at the periphery that have been proven to prevent infection of free HIV-1 *in vitro*. These dendrimers have been prepared *via* hydrosilylation reaction followed by a Michael-type addition reaction<sup>8</sup> or using a

<sup>a</sup>Departamento de Química Inorgánica, Universidad de Alcalá, Campus Universitario, E-28871 Alcalá de Henares, Spain

<sup>b</sup>Networking Research Center on Bioengineering, Biomaterials and Nanomedicine (CIBER-BBN), Spain. E-mail: rafael.gomez@uah.es; Fax: (+34) 91 885 4683; Tel: (+34) 91 885 4685

<sup>c</sup>Plataforma de Laboratorio, Hospital General Universitario Gregorio Marañón, Madrid, Spain

<sup>d</sup>Laboratorio de Inmunobiología Molecular, Hospital General Universitario Gregorio Marañón, Madrid, Spain

<sup>e</sup>Faculty of Science, J. E. Purkinje University in Usti n. L., Czech Republic

<sup>f</sup>University of Applied Science of Southern Switzerland, Department of Innovative Technologies, SUPSI-DTI Galleria 2, CH-6928 Manno, Switzerland

†Electronic supplementary information (ESI) available. See DOI: 10.1039/c4ob00162a

click chemistry approach based on the azide–alkyne coupling reaction.<sup>9</sup> However, in the case of the hydrosilylation reaction the synthesis of these nanomolecules is time-consuming, requires drastic reaction conditions which allow side reactions to happen and reaction conditions which are sometimes difficult to transfer from one generation to another. An additional problem is the use of platinum as a catalyst in the process, since it is difficult to remove from the dendritic structure afterwards, especially in higher generations. The azide–alkyne coupling reaction presents a similar problem with the elimination of copper used as catalyst, which might become a drawback from a toxicological point of view.

Therefore, we have focused our work on the development of new synthetic strategies bypassing the use of metals as catalysts and reducing the number of reaction steps and the reaction time whilst maintaining antiviral capacity. One of these protocols is based on thiol–ene chemistry which has the advantages of click reactions (*i.e.* no by-products, compatible with many functional groups,<sup>10</sup> *etc.*). No metal catalyst is used in these reactions, but an organic radical photoinitiator that can be easily removed by conventional methods (*i.e.* by washing or nanofiltration). Herein, we present the synthesis and structural behaviour of a new family of anionic carbosilane dendrimers synthesized *via* thiol–ene methodology as a metal-free approach, which needs few steps and short reaction times. Their application as antiviral agents against HIV is also discussed.

## Results and discussion

The synthesis of the allyl-terminated carbosilane dendrimers has been described elsewhere.<sup>11</sup> These precursors were treated with commercially available thiols under UV-light to provide the functionalized dendrimers in a 4 hour reaction time, in a similar way to that reported by Rissing *et al.*<sup>10c,d</sup> for the synthesis of small ionic compounds from tetravinylsilane. The obtained dendrimers were characterized by <sup>1</sup>H, <sup>13</sup>C and <sup>29</sup>Si NMR, as well as by elemental analysis and mass spectroscopy when possible.

### Sulfonate-terminated dendrimers

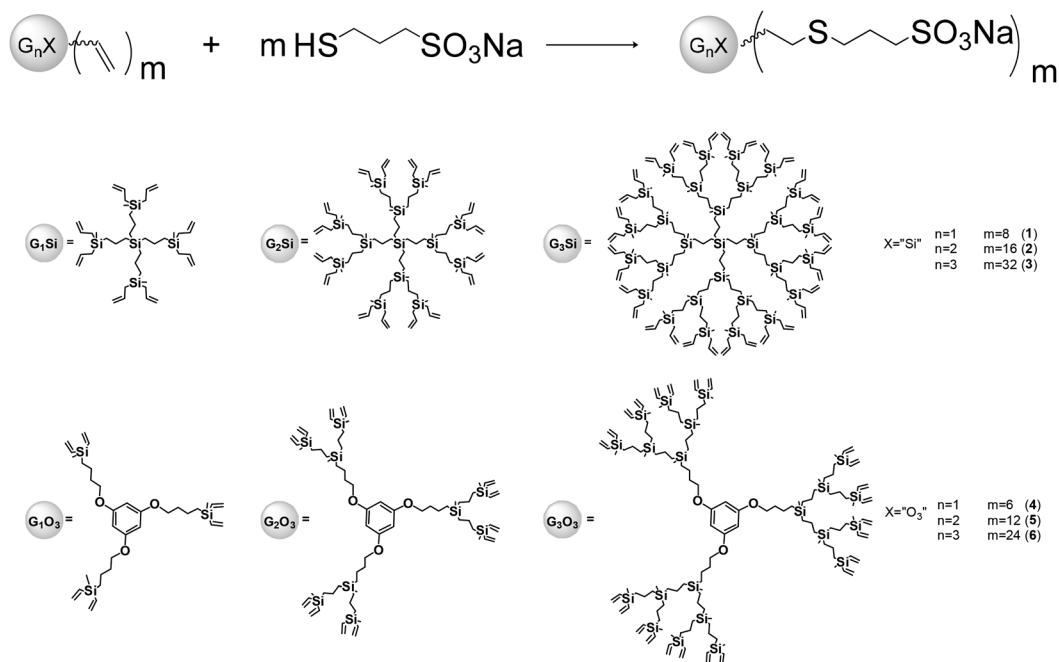
A new family of sulfonate-terminated dendrimers has been designed, attaching this functionality to the carbosilane dendrimer scaffold. The synthetic procedure is based on the radical addition of the thiol derivative to the double bond function of the spherical dendrimer. Allyl-terminated carbosilane dendrimers with a G<sub>n</sub>SiA<sub>m</sub>-type silicon core ( $n = 1, m = 8$ ;  $n = 2, m = 16$  and  $n = 3, m = 32$ , where “Si” means a silicon-cored structure and A<sub>m</sub> is the number of terminal allyl groups)<sup>11</sup> or vinyl-terminated dendrimers, analogue to the allyl-terminated dendrimers previously described by our group<sup>12</sup> with a polyphenoxo core G<sub>n</sub>O<sub>3</sub>V<sub>m</sub> ( $n = 1, m = 6$ ;  $n = 2, m = 12$  and  $n = 3, m = 24$ , where “O<sub>3</sub>” stands for the polyphenoxo-cored structure and V<sub>m</sub> is the number of terminal vinyl groups) were treated with commercially available sodium 3-mercapto-

1-propanesulfonate to afford high yields of {G<sub>n</sub>Si-[S(CH<sub>2</sub>)<sub>3</sub>(SO<sub>3</sub>Na)<sub>m</sub>]} (where  $n = 1, m = 8$  (1);  $n = 2, m = 16$  (2) and  $n = 3, m = 32$  (3)) and {G<sub>n</sub>O<sub>3</sub>[S(CH<sub>2</sub>)<sub>3</sub>(SO<sub>3</sub>Na)<sub>m</sub>]} (where  $n = 1, m = 6$  (4);  $n = 2, m = 12$  (5) and  $n = 3, m = 24$  (6)), respectively. The reactions were performed by stepwise addition of the commercial mercaptosulfonate sodium salt along with a photoinitiator (2,2-dimethoxy-2-phenylacetophenone, DMPA) in a solvent mixture of THF–MeOH–H<sub>2</sub>O under 365 nm UV-light for 4 hours. In each case, the resulting solutions were purified by nanofiltration through appropriate molecular weight cut-off membranes (MWCO = 500 or 1000 Da), and the solvent eliminated by evaporation obtaining the desired dendrimers in moderate yields as white-yellow solids. In cases where the photoinitiator was retained inside the dendritic structure, nanofiltration was not efficient enough and products had to be resuspended in a mixture of MeOH–Et<sub>2</sub>O and subsequently filtered for complete removal of DMPA. All products were soluble in water and low generations were also soluble in MeOH. When considering vinyl-terminated dendrimers, reactions took place under milder conditions, *i.e.* at lower photoinitiator concentration.

The different solubility of the reagents and the products led to the formation of carbosilane dendrimer aggregates subsequently affording lower yields, when the reaction conditions were not specifically adjusted. These problems were solved by adding small amounts of THF to the turbid mixture until complete dissolution and by adding reagents in four steps, in order to avoid aggregate formation due to an increase in ionic strength or a change of pH.<sup>13</sup> The analytical and NMR spectroscopic data of compounds 1–6 are consistent with the proposed structures (see Scheme 1 and Fig. 3).

Herein, only NMR data of the outer sphere will be dealt with, since the carbosilane skeleton has already been described elsewhere<sup>8c,12</sup> and did not undergo modification upon peripheral functionalization. For compounds 1–3, the three signals due to the presence of allyl groups disappeared indicating that the reaction was complete. The <sup>1</sup>H-NMR spectra in D<sub>2</sub>O, however, showed a new chain assigned to three methylene groups at *ca.* 2.60–2.65 ppm for the sulfur-bonded methylene, 1.60–1.66 ppm for the one in β to the sulfur atom and 0.60–0.65 ppm for the methylene group bonded to the silicon atom which can only be assigned with further experiments such as TOCSY and HSQC, since the peaks overlap with the carbosilane scaffold signals. Along with this new chain, three new methylene groups at *ca.* 3.00, 2.70 and 2.00 ppm confirmed the presence of propanesulfonate units, corresponding to the methylene groups in α, γ and β to the sulfonate group, respectively. <sup>13</sup>C-NMR data were also consistent with the proposed structures. The most significant resonances were those attributed to the methylene group attached to sulfonate units (f) that were detected at *ca.* 50 ppm and those bonded to the inner sulfur atom (c) and (d) located at *ca.* 35 and 30 ppm, respectively. As an example, <sup>1</sup>H- and <sup>13</sup>C-NMR spectra of compound 1 in D<sub>2</sub>O are shown in Fig. 1.

For compounds 4–6, only two groups of signals disappeared due to the presence of vinyl groups indicating reaction com-



**Scheme 1** Synthetic pathway and proposed dendritic skeletons for dendrimers 1–6, where "Si" or "O<sub>3</sub>" stand for silicon-cored or polyphenoxo-cored carbosilane structures, respectively.

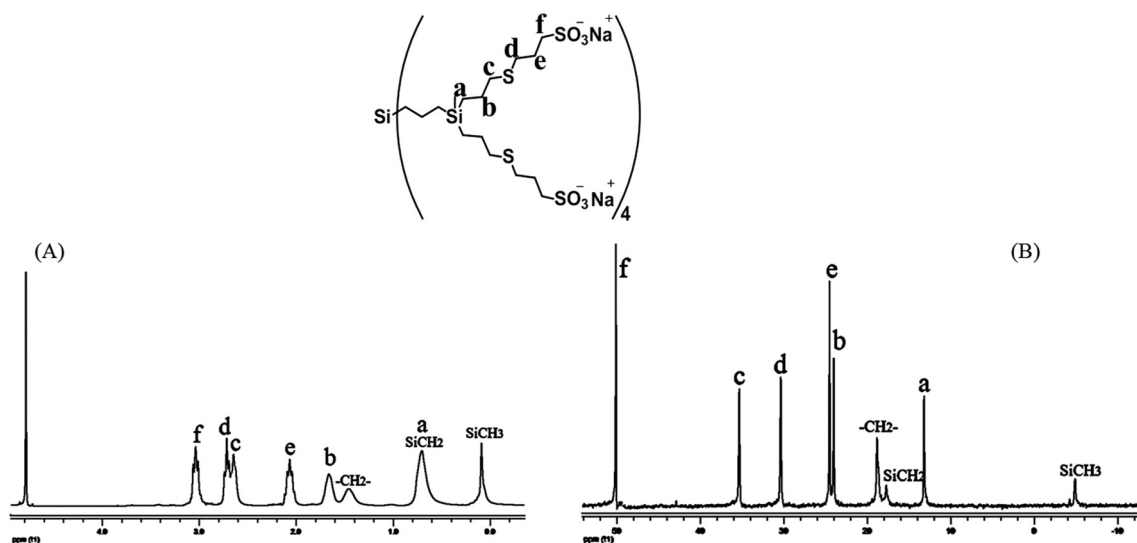


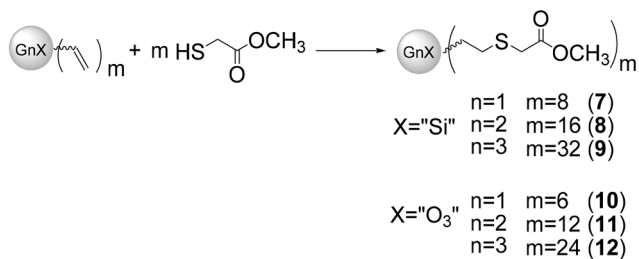
**Fig. 1** NMR data of the first generation dendrimer  $\{G_1\text{Si}[\text{S}(\text{CH}_2)_3(\text{SO}_3\text{Na})_8]\}$  (1), (A)  $^1\text{H}$ -NMR ( $\text{D}_2\text{O}$ ) and (B)  $^{13}\text{C}$ -NMR ( $\text{D}_2\text{O}$ ).

pletion. Analogously, in the  $^1\text{H}$ -NMR spectra, a new chain of two methylene groups appeared at 2.68 and 0.92 ppm. The lower field location of the methylene group bonded to the silicon atom compared with that of the analogue group for the allyl derivatives was due to the presence of the sulfur atom, drawing the chemical shifts to higher ppm values. Three new methylene groups at *ca.* 3.00, again 2.68 and 2.01 ppm confirmed the presence of propanesulfonate units. The  $^{13}\text{C}$ -NMR data were also consistent with the proposed structures, with similar shifts to those observed in derivatives 1–3. Only the methylene group bonded to the silicon atom shifted to a

higher field at *ca.* 14 ppm. The chemical shifts hardly differed from one generation to another, though a broadening of the signals was observed in both types of anionic dendrimers.

#### Methylacrylate-terminated dendrimers

In a synthetic procedure similar to the one described above, the addition of methyl thioglycolate to the same double bonds of functionalized carbosilane dendrimers generated methylacrylate-terminated structures. The reaction was carried out in the presence of THF as solvent and no photoinitiator was needed. Completion of the reaction occurred under UV-light in



Scheme 2 Synthetic pathway for dendrimers 7–12.

shorter times (less than 2 hours) but was highly dependent on the amount of solvent used. A stepwise addition was not necessary in this case. Thus, quantitative yields of  $[\text{G}_n\text{Si}(\text{SCH}_2\text{CO}_2\text{Me})_m]$  (where  $n = 1, m = 8$  (7);  $n = 2, m = 16$  (8) and  $n = 3, m = 32$  (9)) and  $[\text{G}_n\text{O}_3(\text{SCH}_2\text{CO}_2\text{Me})_m]$  (where  $n = 1, m = 6$  (10);  $n = 2, m = 12$  (11) and  $n = 3, m = 24$  (12)) were synthesized

using  $\text{G}_n\text{SiA}_m$  and  $\text{G}_n\text{O}_3\text{V}_m$  as precursors, respectively (see Scheme 2 and Fig. 3).

In this case, the  $^1\text{H-NMR}$  spectra in  $\text{CDCl}_3$  presented two new singlets, one for the methylene group located between the sulfur atom and the carbonyl group  $\text{SCH}_2\text{CO}$  at *ca.* 3.2 ppm and another one as a result of the methylester located at *ca.* 3.7 ppm. The disappearance of the double bond multiplet was used to monitor the reaction's progress. In the  $^{13}\text{C-NMR}$  spectra, the most significant signals were the methoxy group at *ca.* 52.2 ppm and the methylene attributed to the  $\text{SCH}_2\text{CO}$  group at *ca.* 33 ppm for all derivatives while the carbonyl group was located at 171 ppm. The other methylene group bonded to a sulfur atom appeared at 36 and 28 ppm for the silicon and polyphenoxo core derivatives, respectively. The higher field signal observed in the latter ones is attributed to the presence of a silicon atom in  $\beta$  for these compounds. Fig. 2 shows  $^1\text{H-}$  and  $^{13}\text{C-NMR}$  spectra in  $\text{CDCl}_3$  recorded for compound 7.

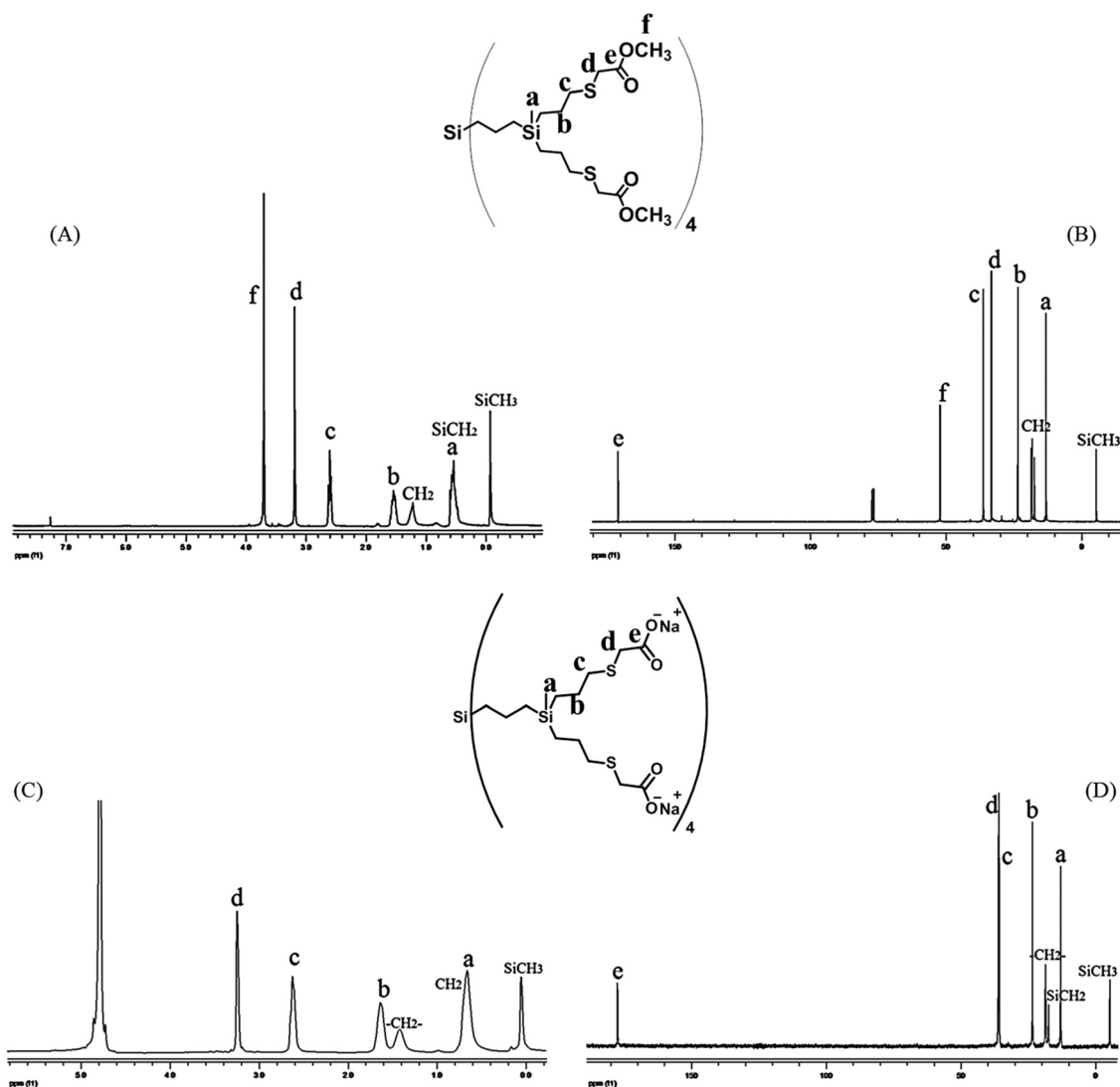


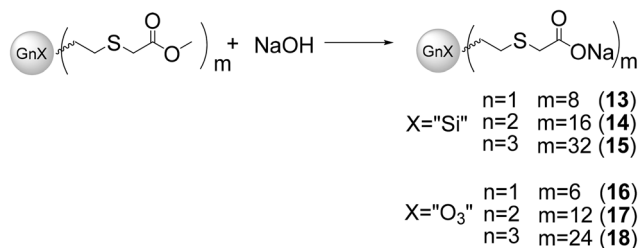
Fig. 2 NMR data of the first generation dendrimers.  $[\text{G}_1\text{Si}(\text{SCH}_2\text{CO}_2\text{Me})_8]$  (7) in  $\text{CDCl}_3$ : (A)  $^1\text{H-NMR}$  and (B)  $^{13}\text{C-NMR}$ .  $[\text{G}_1\text{Si}(\text{SCH}_2\text{CO}_2\text{Na})_6]$  (13) in  $\text{D}_2\text{O}$ : (C)  $^1\text{H-NMR}$  and (D)  $^{13}\text{C-NMR}$ .

### Carboxylate-terminated dendrimers

Carboxylate-terminated dendrimers were easily made from the methylacrylate-terminated systems 7–12 by addition of an excess of NaOH in MeOH leading to precipitation of the desired compounds as white solids. The solvent was removed by filtration and the products were dissolved in water and purified by means of nanofiltration.

The corresponding dendrimers bearing a silicon core [ $G_n\text{Si}(\text{SCH}_2\text{CO}_2\text{Na})_m$ ] (where  $n = 1, m = 8$  (13);  $n = 2, m = 16$  (14) and  $n = 3, m = 32$  (15)) or a polyphenoxo core [ $G_n\text{O}_3(\text{SCH}_2\text{CO}_2\text{Na})_m$ ] (where  $n = 1, m = 6$  (16);  $n = 2, m = 12$  (17) and  $n = 3, m = 24$  (18)) were synthesized in high yields (see Scheme 3 and Fig. 3).

Analysing the NMR data of dendrimers 13–18, a shift to a lower field was observed for the signals of the methylacrylate precursors due to the presence of a negative charge located next to the carboxylate unit. Disappearance of the methylester



Scheme 3 Synthetic pathway for dendrimers 13–18.

resonance in both  $^1\text{H}$  and  $^{13}\text{C}$ -NMR confirmed product formation (see Fig. 2 for an example).

### Molecular modelling

Computer models of the second generation anionic dendrimers (sulfonate 2 and 5, and carboxylate 14 and 17) were

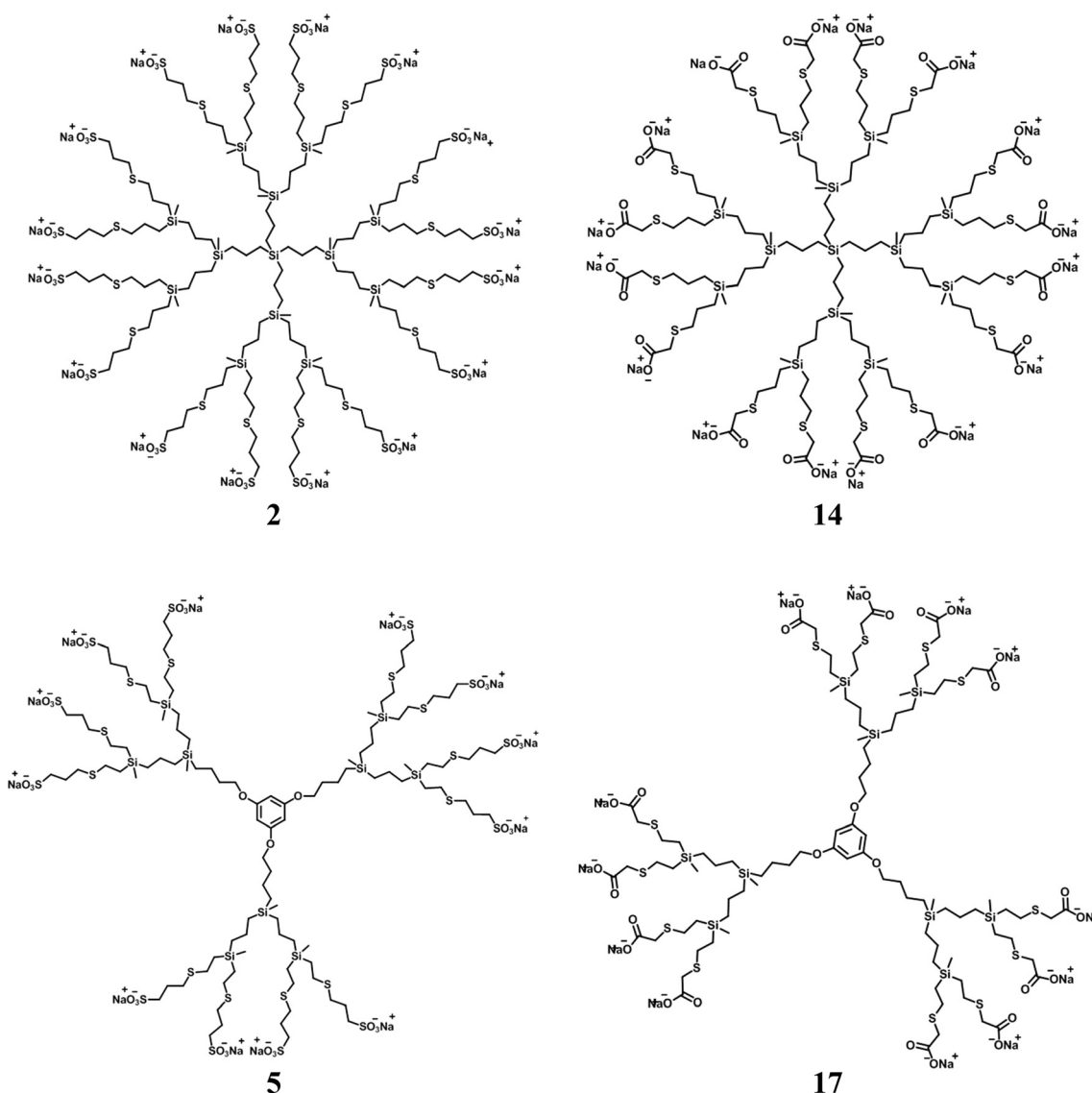
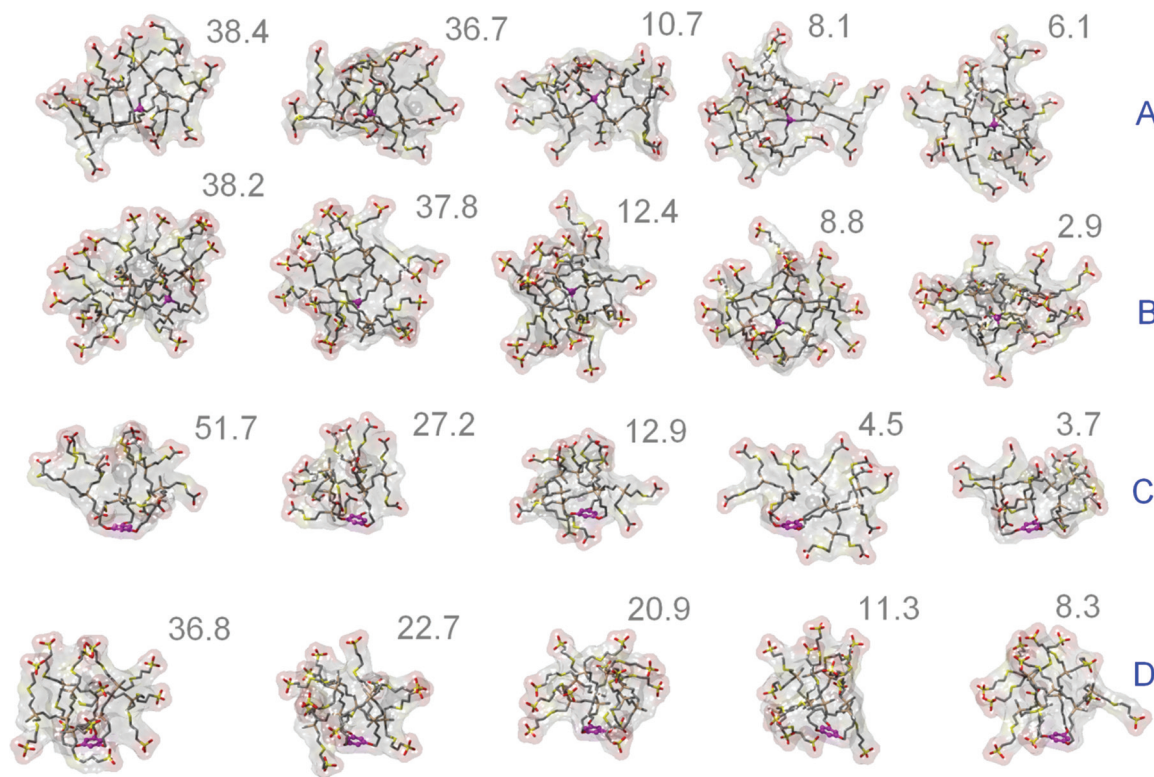


Fig. 3 Molecular representation of second generation dendrimers 2, 5, 14 and 17.



**Fig. 4** The five most representative conformations from the last 50 ns of simulation for each dendrimer, including visualization of the molecular surface. Dendrimers are **14** (A), **2** (B), **17** (C) and **5** (D). The numbers indicate the percentage of all analyzed conformations (5000 conformations obtained from the last 50 ns of simulation) which render best the given representative structures in terms of average RMSD distance (see ESI,† for details). The Si core atom (in **14** and **2**) and phenol ring carbon atoms (in **17** and **5**) are colored in magenta. Hydrogen atoms are omitted for clarity. Atoms are color coded as follows: C – grey, O – red, Si – beige, S – yellow.

created and simulations in explicit salt water were conducted using molecular dynamics in order to get detailed information about their conformation in a water environment at  $T = 310$  K and  $P = 0.1$  MPa. In general, these studies revealed spherical shapes composed of rather shrunken hydrophobic carbosilane interiors surrounded by the hydrophilic terminal groups on the molecular surface (see Fig. 4 and 5).

Equilibrated dendrimer structures were subsequently analyzed. The maximal distance of the dendrimer atoms from the dendrimer center of geometry ( $R_{\max}$ ), which might be interpreted as the highest estimate of the molecular radius, radius of gyration ( $R_g$ ), solvent-accessible surface area (SASA), solvent-excluded surface area (SESA), solvent-excluded volume (SEV), sphericity (SPHER) and conformational variability (CV) were calculated and are shown in Table 1.

From the data presented in Table 1, Fig. 4 and 5 it can be deduced that the structures with the central Si core atom (**14** and **2**) are slightly bigger than those with a polyphenoxo central unit (**17** and **5**). This was particularly clear when structures with different cores but the same terminal groups were compared, which may be mainly attributed to differences in molecular weight (or the total number of atoms present). Regarding the size effect of the terminal groups, the sulfonate structures were larger than the carboxylate ones though bearing the same

core, due to the presence of a longer spacer between the inner sulfur atoms and the terminal anionic groups in the case of sulfonate structures (3 C versus 1 C-long spacer). The difference in size might also be partly attributed to the different interaction of the  $\text{CO}_2^-$  and  $\text{SO}_3^-$  groups with  $\text{Na}^+$  ions and water molecules. From Fig. 6E, the average density of the  $\text{Na}^+$  cations in close proximity to the terminal oxygen atoms (in ca. 2.3 Å distance) was significantly higher for carboxylate groups than for  $\text{SO}_3$ . This fact is connected not only with the different number of oxygen atoms (2 in  $\text{CO}_2$  versus 3 in  $\text{SO}_3$ ) but also with the differences in the nature of the C–O and S–O bonds (electronic structure, length) and in the whole spatial structure of these groups, all of which define an electrostatic field in their close proximity. These aspects determined the way these anionic groups interacted with  $\text{Na}^+$  cations but also with water molecules (see Fig. 7 and from ESI 5†). Therefore,  $\text{Na}^+$  ions, which interacted better with  $\text{CO}_2^-$  groups, played a better “shielding-glueing” role in carboxylated dendrimers than in sulfonated dendrimers, thus contributing to a more compact/flatter surface (see SASA, SESA surface areas, where a flatter/more compact surface should give a smaller area) and also to a smaller molecular size. The tighter spatial packing of  $\text{CO}_2$  groups on the molecular surface was also observed from the radial distribution function of the terminal oxygen atoms (see

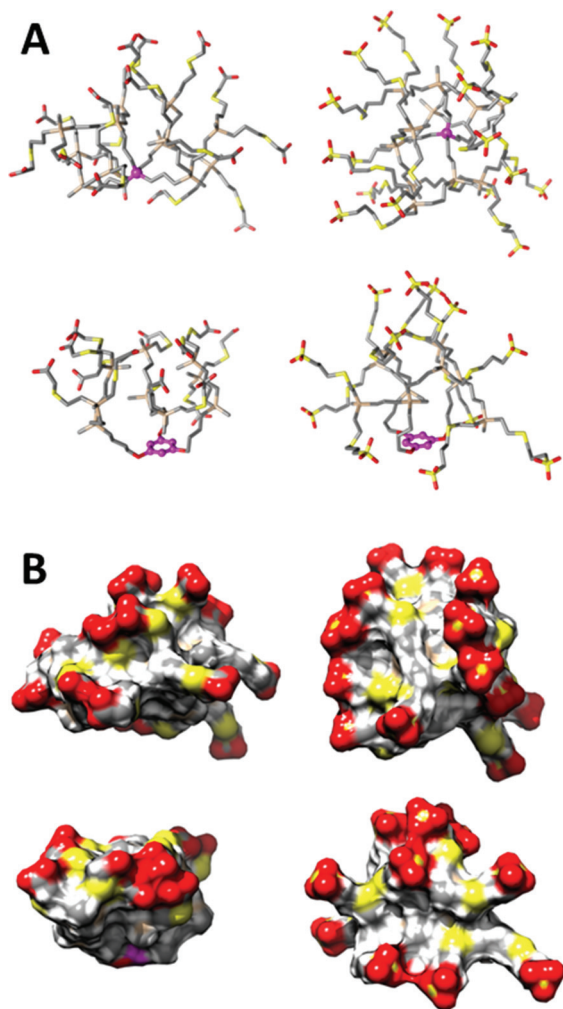


**Fig. 5** Computer models of dendrimers 14 (top-left), 2 (top-right), 17 (bottom-left), 5 (bottom-right) simulated in salt water (A) and their visualized molecular surfaces (B). The Si core atom (in 14 and 2) and phenol ring carbon atoms (in 17 and 5) are colored in magenta. Hydrogen atoms are omitted for clarity. The most representative conformations from the last 50 ns of simulation are shown. Atoms are color coded as follows: C – grey, O – red, Si – beige, S – yellow.

Fig. 6F and ESI† for more data about these interactions). This fact has also been noted in related dendrimers prepared *via* hydrosilylation, as reported elsewhere.<sup>8c</sup>

Analogously, the simulations led us to the conclusion that  $\text{CO}_2^-$  groups also interact better with water molecules (see Fig. ESI 5†) affecting the structure of the first/second water shell and its impact on the dendrimer surface morphology.

As shown in Table 1, the largest molecule was dendrimer 2, with 17 being the smallest. Moreover, dendrimer 17 showed the lowest CV value which means the smallest conformational variability (*i.e.*, the highest stability/rigidity) of its 3D structure (shape) (see also Fig. 4 for corroboration). On the other hand, when comparing dendrimers with the same core but different terminal groups, the sulfonate-terminated systems were more flexible with 5 being the most variable (flexible) structure in salt water but the most spherical one on average. In conclusion, the conformational variability of a given dendrimer depends mainly on the terminal group, with sulfonated dendrimers being conformationally more variable (flexible) than carboxylated ones. This finding might be directly connected with the differences in terminal spacer lengths and interactions with  $\text{Na}^+$  ions and water mentioned above.

When considering the conformational variability between dendrimers with the same terminal groups (see CV values in Table 1), a different behavior was observed depending on their nature. In the case of sulfonate dendrimers, the biggest system 2 had a less variable (*i.e.* more stable) structure than the smaller dendrimer 5. This was probably due to greater steric congestion in 2 resulting from the higher number of available terminal hydrophobic groups. Interestingly, in the case of carboxylate dendrimers the reverse situation was true, though the difference in CV values here is largely negligible.

In order to determine the spatial distribution of different parts in the studied dendrimers (dendrimer atoms, water atoms, C or S atoms from terminal groups or ions) with respect to the dendrimer core, as well as to characterize mutual distributions of some other important atom groups (*e.g.* distribution of  $\text{Na}^+$  ions with respect to the dendrimer terminal oxygen atoms), radial density distribution profiles

**Table 1** Calculated structural parameters.  $R_{\text{max}}$  – the maximal distance of the dendrimer atoms from the dendrimer center of geometry.  $R_g$  – radius of gyration. SASA – solvent-accessible surface area. SESA – solvent-excluded surface area. SEV – solvent-excluded volume. SPHER – sphericity. CV – conformational variability, average distance (RMSD based) between pairs of structures (of the given dendrimer type) (see ESI for details†)

Dendrimer	Si atom core		Polyphenoxo core	
	Carboxylate 14	Sulfonate 2	Carboxylate 17	Sulfonate 5
$R_{\text{max}}$ [nm]	1.7 ± 0.132	1.782 ± 0.125	1.503 ± 0.133	1.621 ± 0.144
$R_g$ [nm]	0.9 ± 0.0277	0.941 ± 0.022	0.793 ± 0.032	0.857 ± 0.026
SASA [nm <sup>2</sup> ]	29.703 ± 1.081	35.137 ± 1.111	23.518 ± 0.712	29.099 ± 1.581
SESA [nm <sup>2</sup> ]	21.944 ± 0.721	26.26 ± 0.884	16.945 ± 0.523	21.031 ± 1.125
SEV [nm <sup>3</sup> ]	3.467 ± 0.027	4.4036 ± 0.044	2.489 ± 0.042	3.132 ± 0.037
SPHER	0.933 ± 0.02	0.948 ± 0.023	0.934 ± 0.031	0.964 ± 0.017
CV [nm]	0.713 ± 0.144	0.745 ± 0.157	0.6983 ± 0.1571	0.8075 ± 0.1654

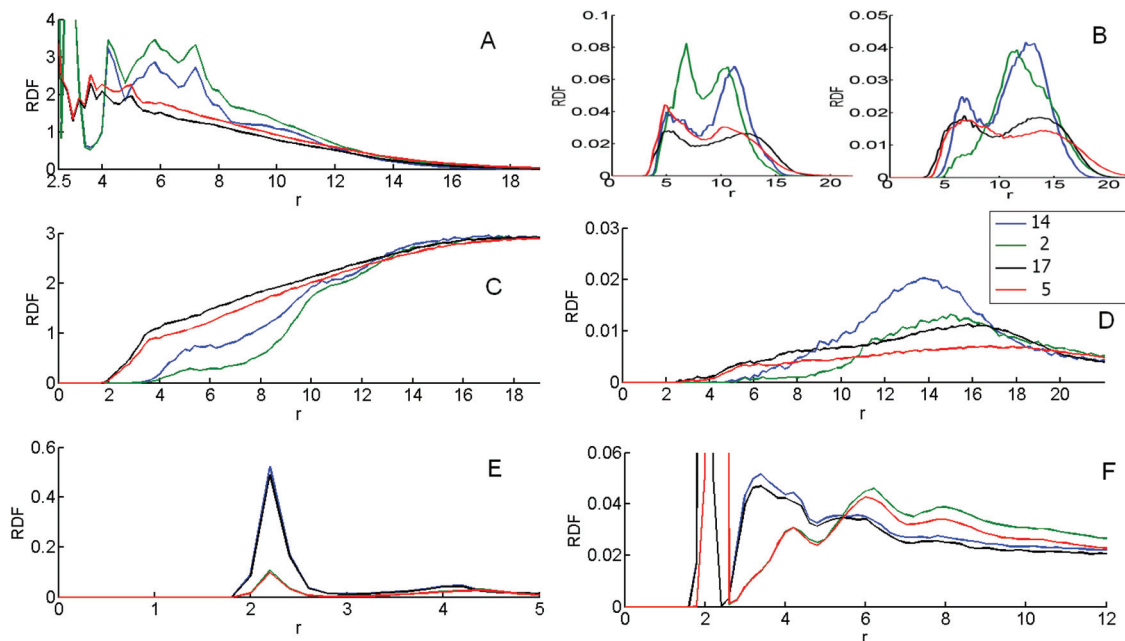


**Fig. 6** Radial distribution density profiles of all dendrimer atoms (A), non-terminal (non-SO<sub>3</sub>) sulfur atoms (left graph in B) and terminal C or S atoms (from carboxylate or sulfonate groups) (right graph in B), water atoms (C) and Na<sup>+</sup> ions (D), in all cases with respect to selected dendrimer core atoms (central Si atom or six C atoms of the polyphenol ring). Radial distribution density profiles of Na<sup>+</sup> ions with respect to terminal oxygen atoms (E) and terminal oxygen atoms with respect to themselves (F). Radial distance *r* measured in Å.

were calculated. The first series of density profiles were calculated taking into account the dendrimer core (central Si atom or six C atoms of the polyphenol ring – colored in magenta in Fig. 4 and 5). These profiles comprised the distribution of all dendrimer atoms, terminal C atoms (of the carboxylate groups) or S atoms (of the SO<sub>3</sub><sup>−</sup> groups but also the non-terminal ones), water atoms and Na<sup>+</sup> ions, and results are shown in Fig. 6.

Fig. 6A shows that the dendrimers with the same core produced similar RDF profiles which means that the overall conformation of solvated dendrimers mainly depends on the architecture of their core and also on associated structural differences. The variation in terminal groups (CO<sub>2</sub><sup>−</sup>, SO<sub>3</sub><sup>−</sup>) induced only minor differences here, which were nevertheless significant in structures bearing the central Si atom at a distance ranging 5–10 Å. The latter might be connected with the fact that **14** preferred a slightly more eccentric position of the central Si atom when compared with **2** (see Fig. 1A and ESI 1†). This is clearly consistent with the water density profiles (see Fig. 3C) where the better accessibility of the solvent to the more eccentric **14** central atom was clearly demonstrated by distinctly higher water density values. In the case of **5** and **17**, the values of water density profiles near the core were noticeably higher thanks to the significantly eccentric core position (providing good accessibility for the solvent).

The differences in the core position were also confirmed by the profiles of the terminal carbon or sulfur atoms (see right graph of Fig. 6B and ESI 1 and 2†). Interestingly, the sharp peak of the non-terminal sulfur atoms profile in dendrimer **2**, centered at about 7.5 Å (see left part of Fig. 6B), revealed

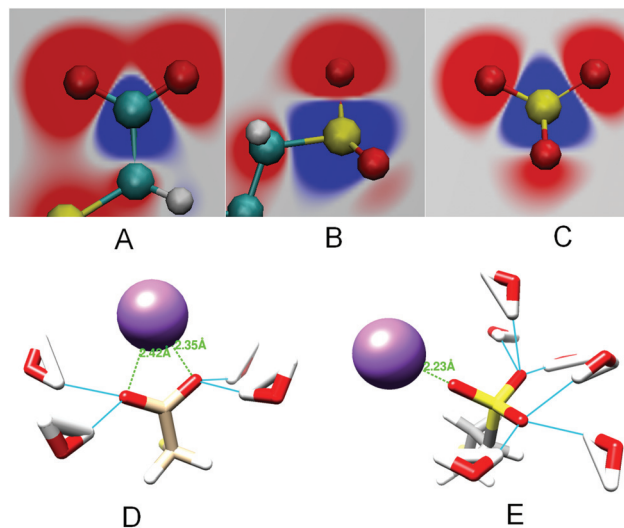


**Fig. 7** Top – electrostatic potential around the CO<sub>2</sub> (A) and SO<sub>3</sub> (B, C) groups. In case A, the plane visualizing the electrostatic potential is defined by the 3 atoms of the CO<sub>2</sub> group. In case B this plane is defined by the last carbon atom, sulfur atom and one oxygen atom (the top one here). In case C the two oxygen atoms (the top ones) and the sulfur atom define the given plane. Atoms are color coded with C in “dark cyan”, O in red, S in yellow and H in white. Regarding potential, the red color denotes low values (−2.57 V and lower) and the blue color means high potential values (+2.57 V and higher). The effect of water was implicitly taken into account in this electrostatic calculation. Bottom – the most favorable/frequent position of the Na<sup>+</sup> (in purple) cation with respect to “isolated” CO<sub>2</sub> (D) and SO<sub>3</sub> (E) groups. The cyan lines denote H-bonds and the green dashed lines together with the green numbers denote O...Na<sup>+</sup> distances. The term “isolated” is used here to indicate a terminal group which is not part of some terminal group cluster sharing one or more Na<sup>+</sup> ions.

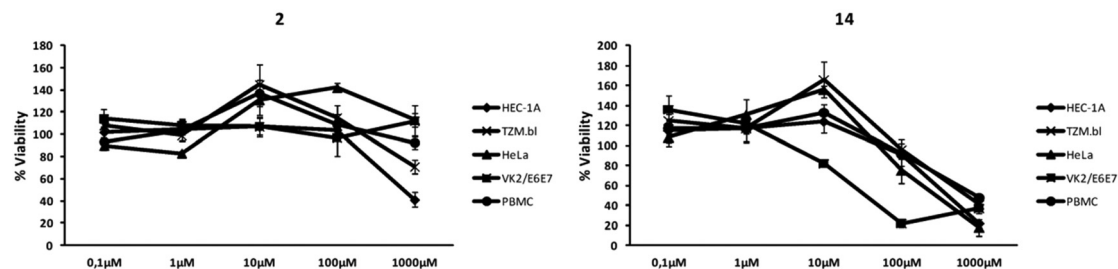


Fig. 8 Viability studies of dendrimers 2 and 14. MTS assay on HEC-1A, TZM.bl, HeLa and VK2/E6E7 cells lines and PBMC after 24 h of incubation.

partial backfolding of some branches. However, this phenomenon did not significantly affect the radial distribution of the hydrophilic terminal groups with respect to the core Si atom due to the relatively long spacer between the non-terminal and the terminal sulfur atoms.

The differences in core eccentricity could be a feature to take into consideration, among others, for the explanation of the different toxicity shown by these systems (*vide infra*). In dendrimers 5 and 17, the higher accessibility of the polyphenoxo core to the biological medium could partially explain the lower biocompatibility when compared with the silicon-cored dendrimers. In addition, the same could be true for the subtle differences observed between the carboxylate dendrimer 14 and the sulfonate system 2.

Regarding the differences between dendrimers prepared by click thiol-ene or Michael-type addition<sup>8</sup> reactions, although the structural parameters like SASA, SESA or SPHER are basically the same, the SEV parameter is always bigger for dendrimers with a sulfur atom than for those reported *via* Michael type addition. The bigger solvent-excluded volume can be related to a higher hydrophobicity of these compounds lacking N atoms. Higher hydrophobicity can also be explained by the lower density profile of water molecules in the internal cavities of dendrimers with S atoms, both for polyphenoxo or silicon cores. The hydrophobicity degree could be an important factor to tune the interaction of dendrimers with biological membranes and therefore with viral or cell receptors. In addition, if radial distribution density profiles are compared between click thiol-ene and Michael-type addition reactions, differences on the eccentricity were observed for dendrimers with polyphenoxo cores (regardless of the synthetic route employed). Also, some eccentricity appears for dendrimer 14 as mentioned above, and not for the equivalent dendrimer obtained through Michael-type addition, which could be explained in terms of the smaller flexibility of the branches of dendrimer 14. Therefore, these data would contribute to understanding the different results observed in terms of toxicity with the different dendrimers used in this work and those reported elsewhere.<sup>8</sup>

### Biomedical assays

Preliminary biomedical experiments were carried out to determine whether the synthesized dendrimers behave as potential candidates for their use in an anti-HIV microbicide formulation.

**Biocompatibility of carbosilane dendrimers.** The biocompatibility assays testing the anionic (carboxylate and sulfonate) carbosilane dendrimers containing both silicon and polyphenoxo cores were carried out using the endometrial epithelial cell line HEC-1A and the human vaginal mucosa cell line VK2/E6E7 as models for the first barrier of protection against HIV infection in the viral transmission process for *in vitro* tests. Other cell lines, like human epithelial HeLa or TZM.bl and peripheral blood mononuclear cells (PBMC) have also been used.

For silicon-cored carbosilane dendrimers, the toxic effect was studied in MTS assays using only the second generation dendrimers, 2 and 14, as the most representative examples, and compared with those prepared *via* hydrosilylation/Michael-type addition procedures reported elsewhere.<sup>8a,c</sup> The sulfonate-terminated dendrimer 2 was biocompatible at concentrations up to 100 mM in all cell lines tested, while the carboxylate-ended dendrimer 14 showed toxicity in VK2/E6E7 and HeLa at this concentration (see Fig. 8). These data are similar to those observed in dendrimers prepared *via* hydrosilylation/Michael-type addition protocols.<sup>8a,c</sup>

In the case of the polyphenoxo-cored dendrimers containing sulfonate, 4–6, or carboxylate, 16–18, units as terminal groups the toxicity profiles were studied by an MTT assay and showed that all dendrimers were toxic in epithelial cell lines HEC-1A and VK2/E6E7 at 10 mM, but biocompatible in PBMC at all concentrations used (see Fig. 9). The results observed in the epithelial cell lines contrasted with those shown by analogous polyphenoxo-cored dendrimers obtained *via* hydrosilylation/Michael-type addition procedure.<sup>8a,c</sup> The higher toxicity detected for dendrimers 4–6 or 16–18 may be tentatively ascribed, along with other factors, to the presence of a polyphenoxo core as predicted by molecular modelling (*vide supra*). Therefore, the observed toxicity prevents their use in subsequent biomedical experiments and only dendrimers 2 and 14 were chosen to study their potential anti-HIV properties.

### Anti-HIV activity in epithelial cell lines

In spite of the fact that urogenital epithelial cells show a slight level of HIV infection, they are the first line of defense against HIV entry into the organism and the first cells encountered during sexual intercourse. VK2/E6E7 and HEC-1A cell lines were pre-treated with dendrimers 2 or 14 at 10 μM for 1 h,

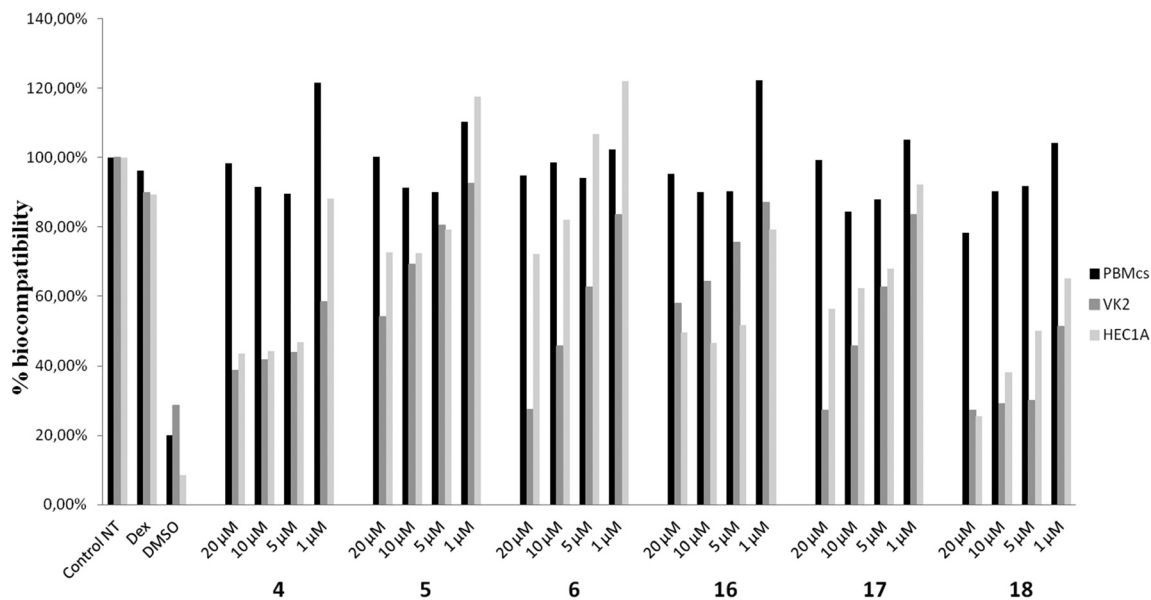


Fig. 9 Biocompatibility studies of dendrimers 4–6 and 16–18 by MTT assay.

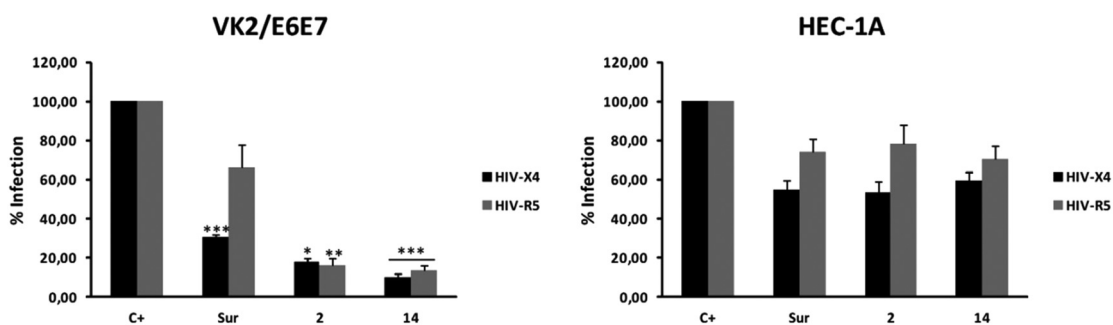


Fig. 10 Anti-HIV activity of dendrimers 2 and 14. VK2/E6E7 (left) and HEC-1A (right) cells were treated with compounds at 10  $\mu\text{M}$ , 1 h before R5-HIV-1<sub>NL(AD8)</sub> or X4-HIV-1<sub>NL4.3</sub> infection. Supernatants were collected after 24 h and p24<sup>gag</sup> antigen levels quantified by ELISA. [Suramin (Sur)] = 10  $\mu\text{M}$ . \* $p$ -value  $\leq 0.01$ ; \*\* $p$ -value  $\leq 0.001$ ; \*\*\* $p$ -value  $\leq 0.0001$  compared with HIV-1 infected non-treated cells (control: C+).

then infected with X4-HIV-1<sub>NL4.3</sub> or R5-HIV-1<sub>NL(AD8)</sub> for 3 h. Suramin was used as positive control of HIV inhibition. Infection of VK2/E6E7 and HEC-1A cell lines was followed by quantification of p24<sup>gag</sup> antigen production in the supernatant of the culture cells after 24 h. An inhibitory effect of p24<sup>gag</sup> antigen production was observed in VK2/E6E7 and HEC-1A when cells were pre-treated with either dendrimer (Fig. 10). Results for VK2/E6E7 showed a significant HIV-1 inhibition when cells were pre-treated with dendrimers 2 or 14 (about 85–90% inhibition) in both viral strains compared with control samples and suramin.

#### Non-inflammatory response: Th1/Th2 cytokine profiles

In order to determine if the treatment with 2 or 14 resulted in changes in the cytokine expression profile that could subsequently activate an inflammatory pathway in neighboring cells, the cytokine profiles of treated VK2/E6E7 cells were analyzed at different times using the Diaplex Human Th1/Th2/

**Table 2** Profile of cytokines secreted by VK2/E6E7. Cells were treated with dendrimer 2 or 14 (10  $\mu\text{M}$ ) for 24 h. Cytokine expression levels were determined in cell culture supernatants by flow cytometry using the Diaplex Human Th1/Th2/inflammation kit. ND: not detected. Poly (inosinic acid–cytidylic acid), (Poly I–C) was used as positive control of cytokine production. Values are expressed in  $\text{pg mL}^{-1}$

Profile of cytokines secreted by VK2/E6E7

VK2/E6E7	Basal	Poly I–C	Dendrimer 2	Dendrimer 14
IL-12	2.75	ND	2.75	2.75
TNF- $\alpha$	17.46	ND	17.46	17.46
IL-4	6.31	ND	6.87	6.87
IL-6	16.75	265.14	16.75	16.75
IL-8	178.05	941.90	351.36	560.36

inflammation kit. The treatment with dendrimers 2 or 14 did not increase expression levels of any cytokine, compared with the medium alone (control cells) (see Table 2). The results

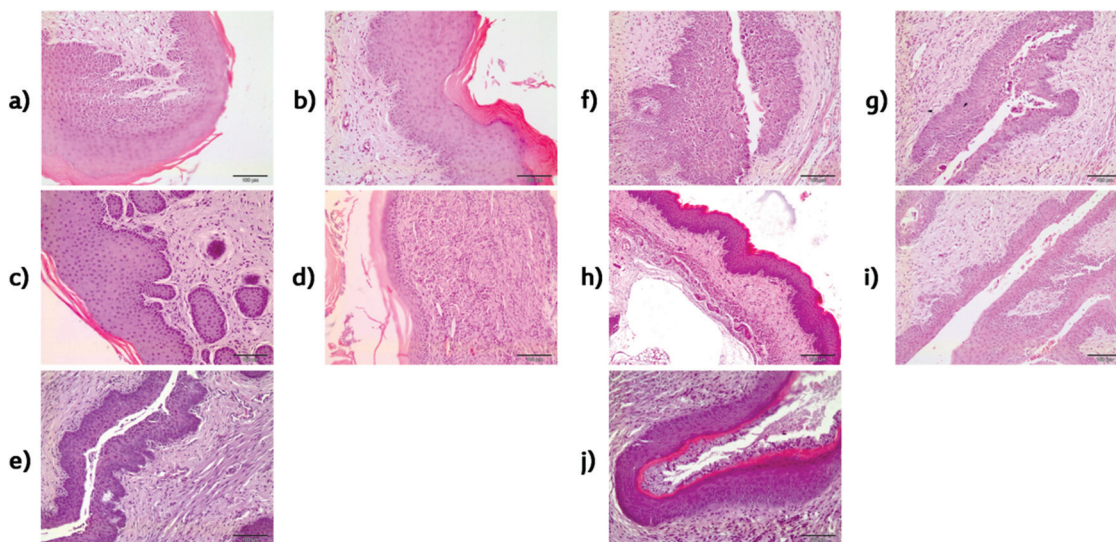


**Fig. 11** Histopathological examination of vaginal tissues after intravaginal application of dendrimers **2** or **14**. Slides were prepared from vaginal tissues treated with **14** LD 2 h (a), **14** HD 2 h (b), **2** LD 2 h (c), **2** HD 2 h (d), vehicle (PBS) 2 h (e), **14** LD 24 h (f), **14** HD 24 h (g), **2** LD 24 h (h), **2** HD 24 h (i), vehicle (PBS) 24 h (j). Hematoxylin-eosin staining was used for all slides. Magnification,  $\times 100$ . LD (low dose,  $10 \mu\text{M}$ ), HD (high dose,  $100 \mu\text{M}$ ).

showed that neither of the dendrimers was able to activate a cellular inflammatory pathway (in case of IL-8, values were not statistically significant)<sup>9</sup> which is essential to make a safe topical microbicide available.

#### Topical vaginal safety in an animal model

The effect of dendrimers **2** and **14** on topical mucosa was studied in a mouse model for *in vivo* evaluation, analyzing the integrity of the mucosal tissue. Histopathological examination showed that dendrimer-treated mice displayed neither damage nor inflammatory response in cervicovaginal tissues (see Fig. 11). No mortality or signs of vaginal discharge, erythema or edema were observed in mice treated with the lowest dose ( $10 \mu\text{M}$ ) and higher dose ( $100 \mu\text{M}$ ) of dendrimers **2** and **14** (see ESI Table 1†). In post-mortem and histopathological examinations of the vaginal tissues, no significant abnormalities were observed in the mucosa in the presence of the dendrimers compared with the vehicle (negative control). The vaginal irritation index was calculated by scoring the microscopic observations (irritation of epithelium, leukocyte infiltration, vascular congestion and edema) and achieved values of 1.7 and 0.3 after 2 h, and 0.3 and 1.3 after 24 h for dendrimer **14** at low and high dose, respectively, and values of 1 and 2 at 2 h, and 2.3 and 2.67 at 24 h for dendrimer **2** at low and high dose, respectively. According to Eckstein *et al.*, a vaginal irritation index  $< 8$  is acceptable, 9–10 is marginal, and  $\geq 11$  unacceptable.<sup>14</sup> These data confirmed the biocompatibility of both dendrimers applied to the vaginal mucosa of mice. Thus, dendrimers **2** and **14** did not induce vaginal irritation and seem to be a safe product for topical application.

## Conclusions

A synthetic strategy has been developed for the preparation of anionic carbosilane dendrimers bearing sulfonate or carboxylate groups at their periphery. It is based on the use of thiol-ene chemistry which offers several advantages over other different synthetic protocols used for preparing similar dendrimers, *e.g.* hydrosilylation reaction followed by a Michael-type addition<sup>8</sup> or alkyne-azide coupling.<sup>9</sup> First of all, this procedure entails fewer reaction steps and milder reaction conditions. While the hydrosilylation protocol requires temperatures ranging between 90–120 °C and long reaction times, normally 2–3 days, and the azide-alkyne procedure is carried out at 40–60 °C and takes at least 24 h, the thiol-ene reactions work at room temperature and require 4 h for completion. In addition, no metal catalyst is used in these reactions, but an organic radical photoinitiator that can easily be removed by conventional methods (*i.e.* by washing or by nanofiltration). Therefore, this synthetic technology offers milder reaction conditions, shorter reaction times and easier purification methods.

Molecular dynamics simulations of the second generation anionic dendrimers bearing a silicon core, **2** and **14**, or a polyphenoxo core, **5** and **17**, were performed in explicit salt water. In general, these studies revealed spherical shapes composed of rather shrunken hydrophobic carbosilane interiors surrounded by the hydrophilic terminal groups on the molecular surface. Regarding the size effect of the terminal groups, the sulfonate structures are bigger and more flexible than the carboxylate ones containing the same core. This can be ascribed to a longer spacer between the inner sulfur atoms and the terminal anionic groups, but also partly attributed to the different interactions of the  $\text{CO}_2^-$  and  $\text{SO}_3^-$  groups with the

Na<sup>+</sup> ions and water molecules. With regard to conformational variability, polyphenoxo-cored dendrimers **5** and **17** show a high core eccentricity which means that in these cases the core is rather close to the molecular surface and therefore more accessible to the solvent. This difference could be linked to the different toxicity shown by these systems when compared with silicon-cored dendrimers. The same may apply for the subtle differences observed between the carboxylate dendrimer **14** and the sulfonate system **2**. From the theoretical analysis, dendrimer **2** presents structural differences that make it more flexible than the corresponding analogous carboxylate system **14**. This property may be very useful for an antiviral agent, since more flexibility means more effectiveness of the surface when interacting with important domains of viral or cellular receptors.

The biocompatibility of anionic carbosilane dendrimers containing either silicon or polyphenoxo cores has been tested on endometrial epithelial cell lines HEC-1A and human vaginal mucosa VK2/E6E7 as models of the first barrier of protection against HIV infection as well as on other cell lines like HeLa or TZM.bl and primary culture PBMC. Silicon-cored dendrimers are non-toxic up to 100 mM, while the polyphenoxo-cored systems show reduced biocompatibility as predicted by molecular modelling studies. For this reason, only silicon-cored second generation dendrimers **2** and **14** were used for HIV antiviral assays, showing 85–90% of inhibition compared with the control and higher values than the positive control suramin in both viral strains, VIH-X4 and HIV-R5. In addition, both dendrimers did not trigger inflammation nor vaginal irritation in mice. These features are important and need to be considered, since creating an inflammatory state may fatally increase viral transmission, as described in the literature on the failure of nonoxinol-9 (N-9) as an anti HIV vaginal microbicide.<sup>15</sup>

Regarding the differences between dendrimers prepared by click thiol–ene or Michael-type addition<sup>8</sup> reactions, the former introduces a sulfur atom in the structure, while a nitrogen atom is present in the latter. The basicity of the inner nitrogen creates zwitterionic species in the case of the carboxylate dendrimers at physiological pH, a situation that cannot occur in analogous dendrimers from the thiol–ene protocol. The existence of non-protonated structures and the conformation adopted by the carboxylate dendrimers and confirmed by molecular modeling may explain the different biomedical behavior observed. The fact that no big differences were found for the sulfonate dendrimers prepared from the two synthetic protocols corroborates the similar biomedical behavior. In addition, the different hydrophobicity and eccentricity values found in dendrimers synthesized by the two protocols should be taken into consideration for biomedical purposes.

Therefore, with these very promising data concerning conformation, biocompatibility, inhibition, non-inflammatory response and integrity of the mucosal tissues against irritation, combined with a clean, simple and metal-free synthetic method based on thiol–ene chemistry, dendrimer **2** and dendrimer **14**, though perhaps to a lesser degree, seem to be

good, safe and readily available candidates for topical vaginal microbicides against HIV. Deeper biomedical studies are in progress in order to further investigate their potential use as microbicide agents.

## Experimental section

### General methods

Unless otherwise stated, reagents were obtained from commercial sources and used as received. Compounds G<sub>n</sub>XY<sub>m</sub> (X = Si, Y = allyl and X = O<sub>3</sub>, Y = vinyl) were synthesized as published.<sup>11,12,16</sup> Thiol–ene reactions were carried out employing a HPK 125W Mercury Lamp from Heraeus Noblelight with maximum energy at 365 nm, in normal glassware under inert atmosphere. NMR spectra were recorded on a Varian Unity VXR-300 (300.13 (<sup>1</sup>H), 75.47 (<sup>13</sup>C) MHz) or on a Bruker AV400 (400.13 (<sup>1</sup>H), 100.60 (<sup>13</sup>C), 79.49 (<sup>29</sup>Si) MHz). Chemical shifts (δ) are given in ppm. <sup>1</sup>H and <sup>13</sup>C resonances were measured relative to solvent peaks considering TMS = 0 ppm, while <sup>29</sup>Si resonances were measured relative to external TMS. When necessary, assignment of resonances was done from HSQC and TOCSY NMR experiments. Elemental analyses were performed on a Perkin-Elmer 240C. Mass Spectra were obtained from an Agilent 6210 (ESI).

### Synthesis of compounds

Dendrimers are named as G<sub>n</sub>XY<sub>m</sub>, where *n* = 1, 2, 3 for first, second and third generation dendrimers respectively; X = Si or O<sub>3</sub> for silicon or polyphenoxo-cored dendrimers and Y<sub>m</sub> = allyl or vinyl groups in the periphery.

Only characterization data for second generation dendrimers are presented here, as they were chosen for molecular modeling and biomedical assays. Complete characterization of all compounds along with synthetic procedure and selected NMR spectra can be found in the ESI.†

**G<sub>2</sub>Si[S(CH<sub>2</sub>)<sub>3</sub>(SO<sub>3</sub>Na)<sub>16</sub>] (2).** C<sub>144</sub>H<sub>300</sub>Na<sub>16</sub>O<sub>48</sub>S<sub>32</sub>Si<sub>13</sub> (4558.92). White powder solid (1.08 g, 80%). **Reagents:** G<sub>2</sub>SiA<sub>16</sub> (0.51 g, 0.29 mmol), sodium 3-mercapto-1-propanesulfonate (1.02 g, 5.73 mmol), DMPA (0.15 g, 0.57 mmol). **<sup>1</sup>H-NMR** (D<sub>2</sub>O): δ 2.99 (32 H, t, SCH<sub>2</sub>CH<sub>2</sub>CH<sub>2</sub>SO<sub>3</sub>Na), 2.66 (32 H, t, SCH<sub>2</sub>CH<sub>2</sub>CH<sub>2</sub>SO<sub>3</sub>Na), 2.59 (32 H, t, SiCH<sub>2</sub>CH<sub>2</sub>CH<sub>2</sub>S), 2.02 (32 H, m, SCH<sub>2</sub>CH<sub>2</sub>CH<sub>2</sub>SO<sub>3</sub>Na), 1.61 (32 H, m, SiCH<sub>2</sub>CH<sub>2</sub>CH<sub>2</sub>S), 1.41 (24 H, m, SiCH<sub>2</sub>CH<sub>2</sub>CH<sub>2</sub>Si), 0.65 (80 H, m, SiCH<sub>2</sub>CH<sub>2</sub>CH<sub>2</sub>Si(Me)CH<sub>2</sub>CH<sub>2</sub>CH<sub>2</sub>S), 0.04 (36 H, s, SiMe). **<sup>13</sup>C-NMR** (D<sub>2</sub>O): δ 50.04 (SCH<sub>2</sub>CH<sub>2</sub>CH<sub>2</sub>SO<sub>3</sub>Na), 35.23 (SiCH<sub>2</sub>CH<sub>2</sub>CH<sub>2</sub>S), 30.27 (SCH<sub>2</sub>CH<sub>2</sub>CH<sub>2</sub>SO<sub>3</sub>Na), 24.44 (SCH<sub>2</sub>CH<sub>2</sub>CH<sub>2</sub>SO<sub>3</sub>Na), 23.93 (SiCH<sub>2</sub>CH<sub>2</sub>CH<sub>2</sub>S), 18.58 (SiCH<sub>2</sub>CH<sub>2</sub>CH<sub>2</sub>Si, SiCH<sub>2</sub>CH<sub>2</sub>CH<sub>2</sub>Si), 13.11 (SiCH<sub>2</sub>CH<sub>2</sub>CH<sub>2</sub>S), −4.26 (SiMe), −5.04 (SiMeCH<sub>2</sub>CH<sub>2</sub>CH<sub>2</sub>S). **<sup>29</sup>Si-RMN** (D<sub>2</sub>O): δ 2.52 (SiMeCH<sub>2</sub>CH<sub>2</sub>CH<sub>2</sub>S), 1.21 (SiMeCH<sub>2</sub>CH<sub>2</sub>CH<sub>2</sub>Si). **Elemental analysis:** Calc. %: C, 37.94; H, 6.63; S, 22.51; exp %: C, 36.54; H, 6.39; S, 23.26.

**G<sub>2</sub>O<sub>3</sub>[S(CH<sub>2</sub>)<sub>3</sub>(SO<sub>3</sub>Na)<sub>12</sub>] (5).** C<sub>105</sub>H<sub>210</sub>Na<sub>12</sub>O<sub>39</sub>S<sub>24</sub>Si<sub>9</sub> (3394.97). White powder solid (0.43 g, 80%). **Reagents:** G<sub>2</sub>O<sub>3</sub>V<sub>12</sub> (0.20 g, 0.16 mmol), sodium 3-mercapto-1-propanesulfonate (0.42 g,

1.92 mmol), DMPA (0.05 g, 0.19 mmol).  $^1\text{H-NMR}$  ( $\text{D}_2\text{O}$ ):  $\delta$  5.98 (3 H, s, ArH), 3.77 (6 H, t,  $\text{CH}_2\text{O}$ ), 2.97 (24 H, t,  $\text{SCH}_2\text{CH}_2\text{CH}_2\text{SO}_3\text{Na}$ ), 2.65 (48 H, m,  $\text{SiCH}_2\text{CH}_2\text{S}$ ,  $\text{SCH}_2\text{CH}_2\text{CH}_2\text{SO}_3\text{Na}$ ), 2.00 (24 H, m,  $\text{SCH}_2\text{CH}_2\text{CH}_2\text{SO}_3\text{Na}$ ), 1.37 (18 H, m,  $\text{OCH}_2\text{CH}_2\text{CH}_2\text{CH}_2\text{Si}$ ,  $\text{SiCH}_2\text{CH}_2\text{CH}_2\text{Si}$ ), 0.92 (24 H, t,  $\text{SiCH}_2\text{CH}_2\text{S}$ ), 0.60 (30 H, m,  $\text{OCH}_2\text{CH}_2\text{CH}_2\text{CH}_2\text{Si}$ ,  $\text{SiCH}_2\text{CH}_2\text{CH}_2\text{Si}$ ), 0.06 (18 H, s,  $\text{SiMeCH}_2\text{CH}_2\text{S}$ ),  $-0.04$  (9 H, s,  $\text{SiMe}$ ).  $^{13}\text{C-NMR}$  ( $\text{D}_2\text{O}$ ):  $\delta$  67.53 ( $\text{OCH}_2$ ), 50.12 ( $\text{SCH}_2\text{CH}_2\text{CH}_2\text{SO}_3\text{Na}$ ), 30.13 ( $\text{SiCH}_2\text{CH}_2\text{S}$ ), 26.96 ( $\text{SCH}_2\text{CH}_2\text{CH}_2\text{SO}_3\text{Na}$ ), 24.34 ( $\text{SCH}_2\text{CH}_2\text{CH}_2\text{SO}_3\text{Na}$ ), 18.52 ( $\text{SiCH}_2\text{CH}_2\text{CH}_2\text{Si}$ ), 14.33 ( $\text{SiCH}_2\text{CH}_2\text{S}$ ,  $\text{SiCH}_2\text{CH}_2\text{CH}_2\text{Si}$ ),  $-4.58$  ( $\text{SiMe}$ ),  $-5.48$  ( $\text{SiMeCH}_2\text{CH}_2\text{S}$ ).  $^{29}\text{Si-RMN}$  ( $\text{D}_2\text{O}$ ):  $\delta$  2.10 ( $\text{SiMeCH}_2\text{CH}_2\text{S}$ ), 1.00 ( $\text{SiMeCH}_2\text{CH}_2\text{CH}_2\text{Si}$ ). **Elemental analysis:** Calc. %: C, 37.15; H, 6.23; S, 22.67; exp %: C, 37.09; H, 6.64; S, 25.51.

$\text{G}_2\text{Si}[(\text{SCH}_2\text{CO}_2\text{Me})_{16}]$  (**8**).  $\text{C}_{144}\text{H}_{284}\text{O}_{32}\text{S}_{16}\text{Si}_{13}$  (3405.93). Oil (0.25 g, 60%). **Reagents:**  $\text{G}_2\text{SiA}_{16}$  (0.22 g, 0.13 mmol), methyl thioglycolate (0.2 mL, 2.02 mmol).  $^1\text{H-NMR}$  ( $\text{CDCl}_3$ ):  $\delta$  3.71 (48 H, s,  $\text{COOCH}_3$ ), 3.19 (32 H, s,  $\text{SCH}_2\text{CO}$ ), 2.62 (32 H, t,  $\text{SiCH}_2\text{CH}_2\text{CH}_2\text{S}$ ), 1.55 (32 H, m,  $\text{SiCH}_2\text{CH}_2\text{CH}_2\text{S}$ ), 1.23 (24 H, m,  $\text{SiCH}_2\text{CH}_2\text{CH}_2\text{Si}$ ), 0.54 (80 H, m,  $\text{SiCH}_2\text{CH}_2\text{CH}_2\text{Si}(\text{Me})\text{CH}_2\text{CH}_2\text{CH}_2\text{S}$ ),  $-0.05$  (24 H, s,  $\text{SiMeCH}_2\text{CH}_2\text{CH}_2\text{S}$ ),  $-0.09$  (12 H, s,  $\text{SiCH}_2\text{CH}_2\text{CH}_2\text{SiMe}$ ).  $^{13}\text{C-NMR}$  ( $\text{CDCl}_3$ ):  $\delta$  170.89 ( $\text{COOCH}_3$ ), 52.30 ( $\text{COOCH}_3$ ), 36.34 ( $\text{SiCH}_2\text{CH}_2\text{CH}_2\text{S}$ ), 33.33 ( $\text{SCH}_2\text{COOCH}_3$ ), 23.66 ( $\text{SiCH}_2\text{CH}_2\text{CH}_2\text{S}$ ), 13.30 ( $\text{SiCH}_2\text{CH}_2\text{CH}_2\text{S}$ ), 18.84–18.36 ( $\text{SiCH}_2\text{CH}_2\text{CH}_2\text{Si}$ ,  $\text{SiCH}_2\text{CH}_2\text{CH}_2\text{Si}$ ),  $-5.25$  ( $\text{SiMe}$ ).  $^{29}\text{Si-NMR}$  ( $\text{CDCl}_3$ ):  $\delta$  2.69 ( $\text{SiMeCH}_2\text{CH}_2\text{CH}_2\text{S}$ ), 0.81 ( $\text{SiCH}_2\text{CH}_2\text{CH}_2\text{SiMe}$ ). **Elemental analysis:** Calc. %: C, 50.78; H, 8.40; S, 15.06; exp %: C, 51.41; H, 7.84; S, 15.09.

$\text{G}_2\text{O}_3[(\text{SCH}_2\text{CO}_2\text{Me})_{12}]$  (**11**).  $\text{C}_{105}\text{H}_{198}\text{O}_{27}\text{S}_{12}\text{Si}_9$  (2526.87). Oil (0.50 g, 80%). **Reagents:**  $\text{G}_2\text{O}_3\text{V}_{12}$  (0.31 g, 0.25 mmol), methyl thioglycolate (0.30 mL, 3.00 mmol).  $^1\text{H-NMR}$  ( $\text{CDCl}_3$ ):  $\delta$  6.02 (3 H, s, Ar-H), 3.86 (6 H, t,  $\text{CH}_2\text{O-Ar}$ ), 3.69 (36 H, s,  $\text{COOCH}_3$ ), 3.21 (24 H, s,  $\text{SCH}_2\text{CO}$ ), 2.63 (24 H, t,  $\text{SiCH}_2\text{CH}_2\text{S}$ ), 1.74 (6 H, m,  $\text{OCH}_2\text{CH}_2\text{CH}_2\text{CH}_2\text{Si}$ ), 1.40–1.20 (18 H, m,  $\text{OCH}_2\text{CH}_2\text{CH}_2\text{CH}_2\text{Si}$ ,  $\text{SiCH}_2\text{CH}_2\text{CH}_2\text{Si}$ ), 0.87 (24 H, m,  $\text{SiCH}_2\text{CH}_2\text{S}$ ), 0.55 (30 H, m,  $\text{OCH}_2\text{CH}_2\text{CH}_2\text{CH}_2\text{Si}$ ,  $\text{SiCH}_2\text{CH}_2\text{CH}_2\text{Si}$ ),  $-0.01$  (18 H, s,  $\text{SiMeCH}_2\text{CH}_2\text{S}$ ),  $-0.08$  (9 H, s,  $\text{SiMe}$ ).  $^{13}\text{C-NMR}$  ( $\text{CDCl}_3$ ):  $\delta$  170.73 ( $\text{COOCH}_3$ ), 160.75 ( $C_{\text{ipso}}$ ), 93.54 (ArC), 67.55 ( $\text{OCH}_2$ ), 52.23 ( $\text{COOCH}_3$ ), 33.18 ( $\text{SCH}_2\text{COOCH}_3$ ), 32.55 ( $\text{OCH}_2\text{CH}_2\text{CH}_2\text{CH}_2\text{Si}$ ), 28.11 ( $\text{SiCH}_2\text{CH}_2\text{S}$ ), 20.46 ( $\text{OCH}_2\text{CH}_2\text{CH}_2\text{CH}_2\text{Si}$ ), 18.58 ( $\text{SiCH}_2\text{CH}_2\text{CH}_2\text{Si}$ ), 13.85 ( $\text{SiCH}_2\text{CH}_2\text{S}$ ,  $\text{OCH}_2\text{CH}_2\text{CH}_2\text{CH}_2\text{Si}$ ),  $-5.21$  ( $\text{SiMe}$ ),  $-5.38$  ( $\text{SiMeCH}_2\text{CH}_2\text{S}$ ).  $^{29}\text{Si-NMR}$  ( $\text{CDCl}_3$ ):  $\delta$  2.40 ( $\text{SiMeCH}_2\text{CH}_2\text{S}$ ), 1.71 ( $\text{SiCH}_2\text{CH}_2\text{CH}_2\text{SiMe}$ ). **Elemental analysis:** Calc. %: C, 49.84; H, 7.89; S, 15.21; exp %: C, 51.43; H, 7.84; S, 15.09. **ESI-MS:**  $[\text{M} + (\text{NH}_4)]^+ = 2546.99$ .

$\text{G}_2\text{Si}[(\text{SCH}_2\text{CO}_2\text{Na})_{16}]$  (**14**).  $\text{C}_{128}\text{H}_{236}\text{Na}_{16}\text{O}_{32}\text{S}_{16}\text{Si}_{13}$  (3533.21). White solid powder (0.21 g, 84%). **Reagents:** **8** (0.24 g, 0.07 mmol), NaOH (0.13 g, 3.36 mmol).  $^1\text{H-NMR}$  ( $\text{D}_2\text{O}$ ):  $\delta$  3.21 (32 H, s,  $\text{SCH}_2\text{CO}$ ), 2.59 (32 H, t,  $\text{SiCH}_2\text{CH}_2\text{CH}_2\text{S}$ ), 1.62 (32 H, m,  $\text{SiCH}_2\text{CH}_2\text{CH}_2\text{S}$ ), 1.40 (24 H, m,  $\text{SiCH}_2\text{CH}_2\text{CH}_2\text{Si}$ ), 0.65 (80 H, m,  $\text{SiCH}_2\text{CH}_2\text{CH}_2\text{Si}(\text{Me})\text{CH}_2\text{CH}_2\text{CH}_2\text{S}$ ), 0.04 (36 H, s,  $\text{SiMe}$ ).  $^{13}\text{C-NMR}$  ( $\text{D}_2\text{O}$ ):  $\delta$  178.12 (CO), 36.93 ( $\text{SCH}_2\text{CO}$ ), 35.93 ( $\text{SiCH}_2\text{CH}_2\text{CH}_2\text{S}$ ), 23.59 ( $\text{SiCH}_2\text{CH}_2\text{CH}_2\text{S}$ ), 18.55 ( $\text{SiCH}_2\text{CH}_2\text{CH}_2\text{S}$ ,  $\text{SiCH}_2\text{CH}_2\text{CH}_2\text{Si}$ ,  $\text{SiCH}_2\text{CH}_2\text{CH}_2\text{Si}$ ), 13.11 ( $\text{SiCH}_2\text{CH}_2\text{CH}_2\text{S}$ ),  $-5.10$  ( $\text{SiMe}$ ). **Elemental analysis:** Calc. %: C, 43.51; H, 6.73; S, 14.52 exp %: C, 41.38; H, 6.73; S, 12.81.

$\text{G}_2\text{O}_3[(\text{SCH}_2\text{CO}_2\text{Na})_{12}]$  (**17**).  $\text{C}_{93}\text{H}_{162}\text{Na}_{12}\text{O}_{27}\text{S}_{12}\text{Si}_9$  (2625.69). White solid powder (0.30 g, 60%). **Reagents:** **11** (0.45 g, 0.18 mmol), NaOH (0.26 g, 6.6 mmol).  $^1\text{H-NMR}$  ( $\text{D}_2\text{O}$ ):  $\delta$  5.94 (3 H, s, Ar-H), 3.76 (6 H, t,  $\text{CH}_2\text{O}$ ), 3.30 (24 H, s,  $\text{SCH}_2\text{CO}$ ), 2.69 (24 H, t,  $\text{SiCH}_2\text{CH}_2\text{S}$ ), 1.69 (6 H, m,  $\text{OCH}_2\text{CH}_2\text{CH}_2\text{CH}_2\text{Si}$ ), 1.43 (18 H, m,  $\text{OCH}_2\text{CH}_2\text{CH}_2\text{CH}_2\text{Si}$ ,  $\text{SiCH}_2\text{CH}_2\text{CH}_2\text{Si}$ ), 0.69 (54 H, m,  $\text{SiCH}_2\text{CH}_2\text{S}$ ,  $\text{OCH}_2\text{CH}_2\text{CH}_2\text{CH}_2\text{Si}$ ,  $\text{SiCH}_2\text{CH}_2\text{CH}_2\text{Si}$ ), 0.13 (18 H, s,  $\text{SiMeCH}_2\text{CH}_2\text{S}$ ), 0.03 (9 H, s,  $\text{SiMe}$ ).  $^{13}\text{C-NMR}$  ( $\text{D}_2\text{O}$ ):  $\delta$  177.98 (CO), 160.52 ( $C_{\text{ipso}}$ ), 93.91 (ArC), 67.18 ( $\text{OCH}_2$ ), 37.08 ( $\text{SCH}_2\text{CO}$ ), 32.92 ( $\text{OCH}_2\text{CH}_2\text{CH}_2\text{CH}_2\text{Si}$ ), 27.83 ( $\text{SiCH}_2\text{CH}_2\text{S}$ ), 18.43 ( $\text{OCH}_2\text{CH}_2\text{CH}_2\text{CH}_2\text{Si}$ ), 14.07 ( $\text{SiCH}_2\text{CH}_2\text{S}$ ,  $\text{OCH}_2\text{CH}_2\text{CH}_2\text{CH}_2\text{Si}$ ),  $-4.67$  ( $\text{SiMeCH}_2\text{CH}_2\text{S}$ ),  $-5.16$  ( $\text{SiMe}$ ).  $^{29}\text{Si-RMN}$  ( $\text{D}_2\text{O}$ ):  $\delta$  2.10 ( $\text{SiMeCH}_2\text{CH}_2\text{S}$ ), 1.70 ( $\text{SiMeCH}_2\text{CH}_2\text{CH}_2\text{Si}$ ). **Elemental analysis:** Calc. %: C, 42.54; H, 6.22; S, 14.65; exp %: C, 40.25; H, 6.05; S, 12.29.

### Computational details

3D computer models of dendrimer structures were created using dendrimer builder as implemented in Materials Studio software package from Accelrys Inc. The individual dendrimer residues were parametrised using Antechamber tool which is part of Amber12 software.<sup>17</sup> For calculation of partial charges AM1-BCC approach was used.<sup>18</sup> GAFF force field (Generalized Amber Force Field) was used for parametrisation of our dendrimer models.<sup>19</sup> The missing bond/angle/torsion terms containing silica atoms were derived from QM calculations. These ff parameters were fitted by minimizing the differences between QM and force field based relative energies of properly chosen molecular fragments using *paramfit* routine from AMBER12 software. 100 conformations of each molecular fragment were used for the force field parameters fitting. QM energies were calculated at MP2/HF/6-31G\*\* level of theory using GAMESS software.<sup>20</sup> Van der Waals parameters for Si were taken from the MM3 force field.<sup>21</sup> The dendrimer structures were solvated in explicit water (TIP3P model) with proper number of counterions and additional salt to preserve neutrality of the whole system and to ensure proper ionic strength (0.15 M).<sup>22</sup> All molecular systems were then minimised in two stages. During the first stage, which served for elimination of all bad molecular contacts, solvated molecules were restrained (restraint constant 5 kcal (mol Å<sup>2</sup>)<sup>-1</sup>) and systems were subjected to 500 steps of steepest descent and 4500 conjugate gradient minimization. This first minimization stage was followed by a second one without any restraint applied to let the dendrimer structures relax in a water environment (2000 steepest descent steps + 5000 steps of conjugate gradient). Then all systems were slowly heated using NVT conditions to achieve the desired temperature (310 K). After heating, all molecular systems were simulated using molecular dynamics in NPT ensemble ( $T = 310$  K and  $P = 0.1$  MPa) for 150 ns. Hydrogens were constrained with the SHAKE algorithm<sup>23</sup> to allow 2 fs time step. Langevin thermostat with collision frequency 2 ps was used for all molecular dynamics runs.<sup>24</sup> The pressure relaxation time for weak-coupling barostat was 2 ps. Particle mesh Ewald method (PME)<sup>25</sup> was used to treat long range electrostatic interactions under periodic conditions with

a direct space cutoff of 10 angstroms. The same cutoff was used for van der Waals interactions. The pmemd.cuda module from Amber12 was used for all the above described simulation steps.<sup>26</sup> For the structural and clustering analyses ( $R_g$ ,  $R_{max}$ , RDF, CV *etc.*) the last 5000 frames (which span the final 50 ns of the whole simulation) were used. Amber modules *ptraj*, *cpptraj* were used to accomplish these analyses. The UCSF Chimera software was used for final visualizations and for calculations of molecular surfaces and volumes.<sup>27</sup> Calculations and visualizations of electrostatic potential around CO<sub>2</sub> and SO<sub>3</sub> groups were done using Adaptive Poisson–Boltzmann Solver as implemented in APBS<sup>28</sup> plugin of VMD.<sup>29</sup> Molecular sphericity was expressed using formula (1) where  $I_x$ ,  $I_y$ ,  $I_z$  are principal moments of inertia which were calculated using symmetry tool in VMD.

$$\text{SPHER} = \frac{\sum_{i \neq j} I_i I_j}{\sum_i I_i^2} \quad i, j = x, y, z \quad (1)$$

The SASA, SESA, SEV and SPHER values reported in Table 1 were evaluated only for each of the 5 most representative structures (see Fig. 5) and the reported values were then calculated as the weighted average ( $k1X1 + k2X2 + k3X3 + k4X4 + k5X5$ ) where the weights  $k1$ ,  $k2$ ,  $k3$ ,  $k4$ ,  $k5$  (statistical relevancy) are listed in Fig. 5 for each dendrimer. The reported value of conformational variability CV was calculated as an average value of the root mean square deviations (RMSD of atom coordinates) of all possible pairs of conformations considering the above mentioned set of 5000 conformations.

## Biomedical methods

**Cells.** Blood samples were obtained from healthy anonymous donors from the transfusion centers of Albacete and Madrid following national guidelines. Peripheral blood mononuclear cells (PBMC) were isolated on a Ficoll-Hypaque density gradient (Rafer, Spain) following the current procedures of Spanish HIV HGM BioBank.<sup>30</sup> PBMC and MT2 were cultured in RPMI 1640 medium (Gibco, UK) supplemented with 10% heat-inactivated FBS, 1% L-glutamine and antibiotic cocktail (125 mg mL<sup>-1</sup> ampicillin, 125 mg mL<sup>-1</sup> cloxacillin and 40 mg mL<sup>-1</sup> gentamicin; Sigma, St-Louis, MO, USA). PBMC were cultured with 60 IU mL<sup>-1</sup> of interleukin-2 (IL-2, Bachem, Switzerland) and stimulated with phytohemagglutinin (PHA, 1 µg mL<sup>-1</sup>, Remel, Santa Fe, USA) for 48 h. VK2/E6E7 (ATCC) is an epithelial cell line derived from normal vaginal mucosa tissue and was grown in serum-free keratinocyte medium (Gibco) supplemented with recombinant human epidermal growth factor (rEGF, 0.2 ng mL<sup>-1</sup>, Immunotools, Friesoythe, Germany), bovine pituitary extract (BPE, 30 µg mL<sup>-1</sup>, Sigma-Aldrich), 1% L-glutamine and antibiotics cocktail. HEC-1A (ATCC) is a epithelial cell line derived from a human endometrial carcinoma (uterus mucosa carcinoma) and was grown in McCoy's 5A Medium Modified (Biochrom AG, Germany) supplemented with 10% FBS and antibiotics cocktail. HeLa cell line is a human epithelial cell line derived from a cervical

adenocarcinoma (NIH AIDS Research and Reference Reagent Program), and was grown in DMEM (Life Technologies, Spain) supplemented with 10% FBS, 1% L-glutamine and antibiotic cocktail. TZM.bl cell line (NIH AIDS Research and Reference Reagent Program), which contains integrated copies of luciferase gene under control of the HIV-1 promoter<sup>31</sup> were cultured in DMEM supplemented with 5% FBS, 1% L-glutamine and antibiotic cocktail.

**Virus production.** Virus stocks were prepared by amplification of X4-HIV-1<sub>NL4.3</sub> in MT-2 cell line (ATCC) and HIV-1<sub>NL(AD8)</sub> by transient transfection of pNL(AD8) in 293 T cell line (ATCC). Physical titers of all HIV viral stocks were evaluated by quantification of HIV p24gag by ELISA kit (Innogenetics, Belgium).

**Reagents.** Reagents used as controls for inhibition of viral replication were: Dextran (Sigma-Aldrich), a harmless molecule that is used as a negative control for toxicity; and Suramin (Sigma-Aldrich), an inhibitor of electrostatic attachment of the V3 region of HIV-1 envelope glycoprotein gp120 to galactosylceramide.<sup>32</sup>

**Cell viability assays.** Cell viability was determined by MTS (Promega, Madison, WI, USA) assay following manufacturer's instructions. We included Dextran to evaluate its innocuous effect in cell cultures, DMSO 10% (Sigma-Aldrich) as positive control of cell death and PBS as negative control. Each experiment was performed in triplicate.

**Inhibition of HIV replication.** VK2/E6E7 and HEC-1A epithelial cells were treated with Suramin (10 µM) as positive controls of HIV-inhibition, **2** or **14** (10 µM). Cells were then infected for 3 h with 100 ng per 10<sup>6</sup> cells of X4-HIV-1<sub>NL4.3</sub> or R5-HIV-1<sub>NL(AD8)</sub> and further extensively washed. After 24 h, supernatant of infected epithelial cells were collected and HIV was measured using the p24gag ELISA kit.

**Th1/Th2 cytokines profile.** VK2/E6E7 were treated for 24 h with **2** or **14** (10 µM) and levels of 10 cytokines (IL-8; IL-6; IL-4; TNF-α; IL-12p70) in cell-free supernatants were quantified by using the DIAplex kit (Th1/Th2/inflammation, GenProbe). Cytokine concentration (represented in pg mL<sup>-1</sup>) was calculated from a standard curve of the corresponding recombinant human cytokine. All the cytometric analyses were performed using FACS Gallios™ Beckman Coulter.

**CD-1 (ICR) mice vaginal irritation study.** We analyzed the effect of dendrimers in CD-1 strain mice (CrI: CD-1 (ICR) BR) (Charles River, France). Vaginal smears were made on the mice; mice in estrus cycle were selected and were inoculated with 30 µL of each of the dendrimers in sterile PBS at concentrations of 10 µM (low dose) and 100 µM (high dose) in the vaginas. At 2 and 24 h mice were sacrificed, the vaginas were taken and fixed in 10% formaldehyde. Three mice per condition were used. The pathological examination was made by the company anaPath (Granada, Spain) accredited by ISO 9001:2008. Epithelial lesions were evaluated considering the existence of hyperplasia or hyperkeratosis, ulceration and/or inflammatory infiltrate in the epithelium. The values assigned were 0: no lesions; 1: minimum lesion; 2: slight injury; 3: moderate injury; 4: severe injury. The procedures were performed in accordance with Directive 2010/63/EU of the European

Parliament and Royal Decree 1201/2005, and were approved by the ethics committee on animal experimentation of Hospital General Universitario Gregorio Marañón.

## Acknowledgements

This work has been supported by grants from CTQ2011-23245 (MINECO) and Consortium NANODENDMED ref S2011/BMD-2351 (CM) to R. G. and UAH2011/EXP-037 (University of Alcalá) to F. J. M. This work was supported by grants from Fondos de Investigación Sanitaria ISCIII (INTRASALUD PI09/02029, P509102669), Fundación Eugenio Rodríguez Pascual Red Temática de Investigación Cooperativa Sanitaria ISCIII (RETIC RD06/0006/0035 and RD12/0017/0037), Red Nacional de Biobancos (RD09/0076/00103), INDISNET S-2011-BMD2332, and FIPSE to M. A. M. F. Programa de Investigación de la Consejería de Sanidad de la Comunidad de Madrid (PI11/00888) to JLJF. Marek Maly gratefully acknowledges project GACR 13-06989S. This study was also supported by CIBER-BBN financed by the Instituto de Salud Carlos III, with assistance from the European Regional Development Fund.

## References

- WHO/UNAIDS Global Report 2013.
- N. S. Padian, A. Buvé, J. Balkus, D. Serwadda and W. Cates Jr., *Lancet*, 2008, **372**, 585–599.
- (a) K. K. Ariën, V. Jaspers and G. Vanham, *Rev. Med. Virol.*, 2011, **21**, 110–133; (b) L. C. du Toit, V. Pillay and Y. E. Choonara, *Adv. Drug Delivery Rev.*, 2010, **62**, 532–546; (c) J. Nuttall, *Drugs*, 2010, **70**, 1231–1243.
- M. Lüscher-Mattli, *Antivir. Chem. Chemother.*, 2000, **11**, 249–259.
- (a) B. Cutler and J. Justman, *Lancet Infect. Dis.*, 2008, **8**, 685–697; (b) V. Dzmitruk, D. Shcharbin, E. Pedziwiatr-Werbicka and M. Bryszewska, *Adv. Nanocompos. Technol.*, 2011, 361–374; (c) R. E. Haaland, T. Evans-Strickfaden, A. Holder, C. P. Pau, J. M. McNicholl, S. Chaikummaa, W. Chonwattana and C. E. Hart, *Antimicrob. Agents Chemother.*, 2012, **56**, 3592–3596; (d) A. S. Ham, L. C. Rohan, A. Boczar, L. Yang, K. W. Buckheit and R. W. Buckheit, *Pharm. Res.*, 2012, **29**, 1897–1907; (e) S. Telwatte, K. Moore, A. Johnson, D. Tyssen, J. Sterjovski, M. Aldunate, P. R. Gorry, P. A. Ramsland, G. R. Lewis, J. R. A. Paull, S. Sonza and G. Tachedjian, *Antiviral Res.*, 2011, **90**, 195–199; (f) K. J. Whaley, J. Hanes, R. Shattock, R. A. Cone and D. R. Friend, *Antiviral Res.*, 2010, **88**, S55–S66.
- (a) P. Kissinger, C. R. Cohen, J. Brown, A.-B. Moscicki, E. A. Bukusi, J. R. A. Paull, C. F. Price and S. Shiboski, *PLoS One*, 2011, **6**, e16258; (b) C. F. Price, D. Tyssen, S. Sonza, A. Davie, S. Evans, G. R. Lewis, S. Xia, T. Spelman, P. Hodsman, T. R. Moench, A. Humberstone, J. R. A. Paull and G. Tachedjian, *PLoS One*, 2011, **6**, 1–12; (c) R. Rupp, S. L. Rosenthal and L. R. Stanberry, *Int. J. Nanomedicine*, 2007, **2**, 561–566.
- (a) O. Rolland, C.-O. Turrin, A.-M. Caminade and J.-P. Majoral, *New J. Chem.*, 2009, **33**, 1809; (b) R. Duncan and L. Izzo, *Adv. Drug Delivery Rev.*, 2005, **57**, 2215–2237.
- (a) L. Chonco, M. Pion, E. Vacas, B. Rasines, M. Maly, M. J. Serramía, L. López-Fernández, J. de la Mata, S. Alvarez, R. Gómez and M. A. Muñoz-Fernández, *J. Controlled Release*, 2012, **161**, 949–958; (b) J. L. Jiménez, M. Pion, F. J. D. L. Mata, R. Gomez, E. Muñoz, M. Leal and M. A. Muñoz-Fernandez, *New J. Chem.*, 2012, **36**, 299–309; (c) B. Rasines, J. Sánchez-Nieves, M. Maiolo, M. Maly, L. Chonco, J. L. Jiménez, M. Á. Muñoz-Fernández, F. J. de la Mata and R. Gómez, *Dalton Trans.*, 2012, **41**, 12733–12748.
- (a) E. Vacas-Cordoba, E. Arnaiz, M. Relloso, C. Sanchez-Torres, F. Garcia, L. Perez-Alvarez, R. Gomez, F. J. de la Mata, M. Pion and M. A. Munoz-Fernandez, *AIDS*, 2013, **27**, 1219–1229; (b) E. Arnaiz, E. Vacas-Cordoba, M. Gala, M. Pion, R. Gómez, M. A. Muñoz-Fernandez and F. J. de la Mata, *J. Polym. Sci., Part A. Polym. Chem.*, 2014, **52**, 1099–1112.
- (a) A. Dondoni, *Angew. Chem., Int. Ed.*, 2008, **47**, 8995–8997; (b) K. L. Killips, L. M. Campos and C. J. Hawker, *J. Am. Chem. Soc.*, 2008, **130**, 5062–5064; (c) C. Rissing and D. Y. Son, *Organometallics*, 2008, **27**, 5394–5397; (d) C. Rissing and D. Y. Son, *Organometallics*, 2009, **28**, 3167–3172; (e) R. K. Roy and S. Ramakrishnan, *J. Polym. Sci., Part A: Polym. Chem.*, 2011, **49**, 1735–1744.
- (a) A. W. van der Made, P. W. N. M. van Leeuwen, J. C. De Wilde and R. A. C. Brandes, *Adv. Mater.*, 1993, **5**, 466–468; (b) A. W. van der Made and P. W. N. M. van Leeuwen, *J. Chem. Soc., Chem. Commun.*, 1992, 1400–1401; (c) J. W. J. Knapen, A. W. van der Made, J. C. de Wilde, P. N. M. W. Van Leeuwen, P. Wijkens, D. M. Grove and G. van Koten, *Nature*, 1994, **372**, 659–663; (d) D. Seyferth, D. Y. Son, A. L. Rheingold and R. L. Ostrander, *Organometallics*, 1994, **13**, 2682–2690; (e) G. R. Newkome and C. Shreiner, *Chem. Rev.*, 2010, **110**, 6338–6442.
- J. Sánchez-Nieves, P. Ortega, M. Á. Muñoz-Fernández, R. Gómez and F. J. de la Mata, *Tetrahedron*, 2010, **66**, 9203–9213.
- B. Korthals, M. C. Morant-Miñana, M. Schmid and S. Mecking, *Macromolecules*, 2010, **43**, 8071–8078.
- P. Eckstein, M. C. N. Jackson, N. Millman and A. J. Sobrero, *J. Reprod. Fertil.*, 1969, **20**, 85–93.
- L. Van Damme, G. Ramjee, M. Alary, B. Vuylsteke, V. Chandeying, H. Rees, P. Sirivongrangson, L. Mukenge-Tshibaka, V. Ettiègne-Traoré, C. Uaheowitchai, S. S. Karim, B. Mâsse, J. Perriens and M. Laga, COL-1492 Study Group, *Lancet*, 2002, **360**, 1892–1892.
- A. W. Bosman, H. M. Janssen and E. W. Meijer, *Chem. Rev.*, 1999, **99**, 1665–1688.
- D. A. Case, T. A. Darden, C. T. E. III, C. L. Simmerling, J. Wang, R. E. Duke, R. Luo, R. C. Walker, W. Zhang, K. F. Merz, B. Roberts, S. Hayik, A. Roitberg, G. Seabra, J. Swails, A. W. Goetz, I. Kolossváry, K. F. Wong, F. Paesani, J. Vanicek, R. M. Wolf, J. Liu, X. Wu, S. R. Brozell,

- T. Steinbrecher, H. Gohlke, Q. Cai, X. Ye, J. Wang, M.-J. Hsieh, G. Cui, D. R. Roe, D. H. Mathews, M. G. Seetin, R. Salomon-Ferrer, C. Sagui, V. Babin, T. Luchko, S. Gusarov, A. Kovalenko and P. A. Kollman, University of California, San Francisco, 2012.
- 18 (a) A. Jakalian, D. B. Jack and C. I. Bayly, *J. Comput. Chem.*, 2002, **23**, 1623–1641; (b) A. Jakalian, B. L. Bush, D. B. Jack and C. I. Bayly, *J. Comput. Chem.*, 2000, **21**, 132–146.
- 19 J. Wang, R. M. Wolf, J. W. Caldwell, P. A. Kollman and D. A. Case, *J. Comput. Chem.*, 2004, **25**, 1157–1174.
- 20 (a) M. S. Gordon and M. W. Schmidt, *Theory and Applications of Computational Chemistry: the first forty years*, Elsevier, Amsterdam, 2005; (b) M. W. Schmidt, K. K. Baldridge, J. A. Boatz, S. T. Elbert, M. S. Gordon, J. H. Jensen, S. Koseki, N. Matsunaga, K. A. Nguyen, S. J. Su, T. L. Windus, M. Dupuis and J. A. Montgomery, *J. Comput. Chem.*, 1993, **14**, 1347–1363.
- 21 J.-H. Lii, A. Norman and L. Allinger, *J. Comput. Chem.*, 1991, **12**, 186–199.
- 22 W. L. Jorgensen, J. Chandrasekhar, J. Madura and M. L. Klein, *J. Chem. Phys.*, 1983, **79**, 926.
- 23 J.-P. Ryckaert, G. Ciccotti and H. J. C. Berendsen, *J. Comput. Phys.*, 1977, **23**, 327–341.
- 24 X. Wu and B. R. Brooks, *Chem. Phys. Lett.*, 2003, **381**, 512–518.
- 25 T. Darden, L. Perera, L. Li and L. Pedersen, *Structure*, 1999, **7**, R55–R60.
- 26 A. W. Götz, M. J. Williamson, D. Xu, D. Poole, S. Le Grand and R. C. Walker, *J. Chem. Theory Comput.*, 2012, **8**, 1542–1555.
- 27 E. F. Pettersen, T. D. Goddard, C. C. Huang, G. S. Couch, D. M. Greenblatt, E. C. Meng and T. E. Ferrin, *J. Comput. Chem.*, 2004, **25**, 1605–1612.
- 28 N. A. Baker, D. Sept, S. Joseph, M. J. Holst and J. A. McCammon, *Proc. Natl. Acad. Sci. U. S. A.*, 2001, **98**, 10037–10041.
- 29 W. Humphrey, A. Dalki and K. Schulten, *J. Mol. Graphics*, 1996, **14**, 33–38.
- 30 (a) I. García-Merino, N. de las Cuevas, J. L. Jimenez, J. Gallego, C. Gomez, C. Prieto, M. J. Serramia, R. Lorente, M. A. Munoz-Fernandez and S. H. BioBank, *Retrovirology*, 2009, **6**, 27–37; (b) I. García-Merino, N. de las Cuevas, J. L. Jimenez, A. Garcia, J. Gallego, C. Gomez, D. Garcia and M. A. Muñoz-Fernandez, *AIDS Res. Hum. Retroviruses*, 2010, **26**, 241–244.
- 31 E. J. Platt, M. Bilska, S. L. Kozak, D. Kabat and D. C. Montefiori, *J. Virol.*, 2009, **83**, 8289–8292.
- 32 N. Yahy, J. M. Sabatier, P. Nickel, K. Mabrouk, F. Gonzalezscarano and J. Fantini, *J. Biol. Chem.*, 1994, **269**, 24349–24353.